

# The Affine Divergence: Aligning Activation Updates Beyond Normalisation

George Bird

Department of Computer Science  
& Department of Physics and Astronomy  
University of Manchester

george.bird@postgrad.manchester.ac.uk

December 30, 2025

## Abstract

A systematic mismatch exists between mathematically ideal and effective activation updates during gradient descent. As intended, parameters update in their direction of steepest descent. However, activations are argued to constitute a more directly impactful quantity to prioritise in optimisation, as they are closer to the loss in the computational graph and carry sample-dependent information through the network. Yet their propagated updates do not take the optimal steepest-descent step. These quantities exhibit non-ideal sample-wise scaling across affine, convolutional, and attention layers. Solutions to correct for this are trivial and, entirely incidentally, derive normalisation from first principles despite motivational independence. Consequently, such considerations offer a fresh and conceptual reframe of normalisation’s action, with auxiliary experiments bolstering this mechanistically. Moreover, this analysis makes clear a second possibility: a solution that is functionally distinct from modern normalisations, without scale-invariance, yet remains empirically successful, outperforming conventional normalisers across several tests. This is presented as an alternative to the affine map. This generalises to convolution via a new functional form, “*PatchNorm*”, a compositionally inseparable normaliser. Together, these provide an alternative mechanistic framework that adds to, and counters some of, the discussion of normalisation. Further, it is argued that normalisers are better decomposed into activation-function-like maps with parameterised scaling, thereby aiding the prioritisation of representations during optimisation. Overall, this constitutes a theoretical-principled approach that yields several new functions that are empirically validated and raises questions about the affine + nonlinear approach to model creation.

## 1 Introduction

A deep learning model uses two primary forms of variables to produce the desired outputs. These are the parameters tuned by optimisation, such as weights and biases, and the transient activations/representations, which depend on the specific input, are present in intermediate calculations, and are forward-propagated to the output.

The objective of deep learning is to make stepwise adjustments to such quantities to produce a meaningful output. This is undertaken by backpropagation and an optimiser such as the gradient descent algorithm. Backpropagation computes the gradients of all intermediate quantities with respect to the loss; these gradients represent the direction of steepest descent that changes the loss the fastest with respect to that quantity. This calculation includes both activations and parameters; yet only the gradients of the parameters are used to update the model.

One cannot update the activations directly because they are functions of the input, and this is used to determine their numerical value. Therefore, we update parameters. These become tuned through time, which in turn influences those transient activations, which are then propagated to yield the desired result. Hence, in some respects, parameters are updated as a practical proxy for desired changes in representations.

For gradient descent, parameters are updated by subtracting the gradient of the loss with respect to the parameters, then scaling it by a learning rate scalar. This produces a slight change in the parameters in *their* direction of steepest descent with respect to the loss. For the batch of interest, in the parameter-picture, this is the optimal correction to reduce the loss the fastest.

However, from backpropagation, the optimal steepest direction in which activations should adjust to reduce loss is known. The question becomes: *Does the steepest descent for parameters correspond to the steepest descent for representations when propagated?* The answer is a surprising *no* — even in the simplest of cases.

This constitutes a fundamental and unavoidable structural misalignment in the update step in the *representation space* for affine maps. A divergence arises between the theoretically ideal correction, analytically available from the representation’s gradient, and the effective updates obtained by changing parameters and propagating these corrections to the representations.

Yet, representations more directly influence the loss, carry sample-dependent information and ultimately forward propagate to the overall network output. The question becomes, *why then, is the steepest descent for parameters prioritised whilst representations are neglected to diverge?*. Furthermore, can they be constructed to coincide?

This paper explores the consequences of adapting computations until such an alignment occurs, forming the steepest direction in both parameters and propagated representation corrections. Surprisingly, the solutions to such constraints naturally yield normalisation-like adaptations. Hence, normalisation emerges as a solution, not a premise.

This was unintended and therefore offers a priori derivation naturally yielding normalisers. This may provide a fresh perspective on the success of such implementations in addressing this theoretical ‘affine divergence’. Empirical validation supporting this alternative hypothesis is then provided. Moreover, auxiliary hypotheses are developed indicating that, if this affine divergence mechanism is valid, these new normalisers should, counterintuitively, negatively correlate performance with increases in batch size. This is also empirically validated, adding an independent hypothesis which supports this ‘affine divergence’ as a mechanistic lens on the success of normalisation.

Moreover, such affine divergence solutions are not limited to normalisation-like corrections. A secondary ‘structural’ solution is presented that is neither normalisation-like nor scale-invariant, yet it is empirically successful and outperforms several forms of normalisation across tests. Good performance from this peculiar functional form classically may seem surprising without the affine divergence mechanism. It also provides a theoretical and empirical counterargument that partially undermines scale-invariance as a primary mechanistic cause of empirical success. Overall, this is argued to at least warrant some further discussion.

Following the divergence to the extreme, one could propagate such gradient corrections to the final layer, but this is computationally expensive. However, these considerations are conceptually related to the natural gradient descent approach [1, 2, 3], which considers the Riemannian geometry of the loss. The natural gradient approach can be understood in terms of the contravariant gradient  $\nabla \tilde{\mathcal{L}} = G^{-1} \nabla \mathcal{L}$  with respect to the final loss, in effect prioritising the steepest direction in the model’s output function space instead of parameter space. This induces the Fisher information as the metric to adapt *backpropagated* gradients, and, in turn, the loss decreases more efficiently, in such a way that the steepest descent is invariant to reparameterisations. However, despite conceptual alignment on the suboptimality of classical gradient descent’s direction of steepest descent for the loss, this natural gradient approach differs substantially from the methods presented in this paper in several key ways.

Firstly, the key difference is which quantity’s steepest descent is prioritised with respect to the loss. Classically, these are the parameters, with natural gradients considering the overall model’s output, whilst this work prioritises the intermediate activations for steepest descent. An advantage of this middleground is that the steepest descent for activations is available from backpropagation; moreover, it is trivial to derive analytically. Secondly, this paper discusses two approaches to solving the affine divergence: gradient-only and structural corrections. This paper investigates the latter for various reasons that fundamentally alter the mathematics of the forward pass to align with ideal-effective representation steps. Whereas, if the natural gradient methodology were to be classified in such a picture, it would constitute the former, gradient-based corrections, rather than structural amendments to the network. Thirdly, the Riemannian approach also constitutes a distinct consideration from the ideal-effective argument, which follows from propagated parameter corrections as ‘effective’ changes on subsequent activations. These are two entirely different routes to determine optimality, and they are not mutually exclusive. Hence, although both cases displace the primacy of parameter’s steepest-descent updates, natural gradients are not the same as the present method, with orthogonal implementations that differ in their respective priorities, considerations, and approximations, but do share somewhat overlapping conceptual motivation.

It is argued that the analytical, straightforward ‘structural’ solutions proposed in this paper represent a more computationally tractable middle ground between approaches, which are implementable with simple new transforms. In the process, this simple adjustment to the forward pass maps intended to reproduce the mathematically ideal activation update, in turn elucidates a new derivation and mechanistic explanation for normalisers by happenstance. This novel mechanistic mode may offer a significant and fundamental alternative explanation, and does appeal to covariate shift, variance control, or scale-invariance for motivation.

Overall, this raises several questions, namely, an underappreciated debate regarding which quantities should be given the highest priority in terms of steepest descent. Generally, this constitutes an ideal-effective misalignment in updates, which is applicable widely across deep learning layers<sup>1</sup>. Additionally, it highlights which updates bear the greatest responsibility for providing the affine correction and whether altering this balance of contributions significantly alters the network’s learning. This approach also questions and reimagines the standard affine + nonlinearity construction of models, particularly with their relation to isotropic/anisotropic activation functions [4], as well as the discussion of *App*. A demonstrating an algebraic decomposition of normalisers into activation functions, and several new forms of affine and convolutional layers presented through this work. This arguably dissolves the distinction between what constitutes a

<sup>1</sup>A consideration that developed from prior theoretical discussion [4] regarding the mechanistic explanation of isotropic activation functions’ [5] empirical results.

normaliser and an activation function.

## 2 Theoretical Background

This section begins by providing an overview of the affine divergence, how it arises, and the disparity between the ideal and effective update steps. Then it continues to the implications of such a divergence, the various solutions for its convergence and the interpretation of the newly altered computations.

### 2.1 Deriving The Affine Divergence

This work focuses on the difference between the optimal update for parameters and that for representations, and on how these do not coincide in typical affine layers. This section will begin by showing this divergence. For the majority of what follows, Einstein Summation Convention<sup>2</sup> will be utilised. Additionally, all terms should be evaluated numerically at a particular value, which will be notationally suppressed for straightforward, purely algebraic equations.

Considering the simple affine layer of *Eqn. 1*, and we shall assume for now that the activation function is in a later step, e.g.  $\vec{y} = \mathbf{f}(\vec{z})$ .

$$\vec{z} = \mathbf{W}\vec{x} + \vec{b} \iff z_i = W_{ij}x_j + b_i \quad (1)$$

Then a differentiation with respect to loss,  $\mathcal{L}$ , for each term is undertaken. The shorthand  $\frac{\partial \mathcal{L}}{\partial \vec{z}} \equiv \vec{g}$  is used.

$$\frac{\partial \mathcal{L}}{\partial z_n} = g_n \quad (2)$$

$$\frac{\partial \mathcal{L}}{\partial W_{nm}} = g_n x_m \quad (3)$$

$$\frac{\partial \mathcal{L}}{\partial x_n} = g_i W_{in} \quad (4)$$

$$\frac{\partial \mathcal{L}}{\partial b_n} = g_n \quad (5)$$

These represent the directions of steepest descent for *each* quantity with respect to the loss.

Using these partial derivatives, and substituting them as an update, the optimal gradient step correction for *parameters* is the classical, elementary and familiar gradient descent of *Eqn. 6* and *7*, with learning rate  $\eta$ .

$$W'_{ij} = W_{ij} - \eta \frac{\partial \mathcal{L}}{\partial W_{ij}} \Rightarrow W'_{ij} = W_{ij} - \eta g_i x_j \quad (6)$$

$$b'_i = b_i - \eta \frac{\partial \mathcal{L}}{\partial b_i} \Rightarrow b'_i = b_i - \eta g_i \quad (7)$$

However, as argued, parameters are used as a proxy to update the representations; these are the quantities of interest. But parameter updates are used because representations not only depend on such parameters, but also on the variable input samples; hence, they are not amenable to direct update. Yet, they are indirectly altered through these parameter corrections. Thus, such parameter updates should be propagated to determine the resultant change in representations.

Several crucial approximations are required here. To start, these corrections are first-order in learning rate,  $\eta$ , and also depend on a single-layer approximation, i.e. the propagation begins at each affine layer's parameters and terminates at the affine layer's output activations. This first-order learning rate provides straightforward, tractable solutions and mirrors the first-order gradient information assumed in gradient descent. The single-layer approximation also facilitates simple corrections, as propagating through multiple layers and non-linearities makes such an approach analytically very challenging and would entail excessively complicated considerations. Hence, these approximations are implemented to foreground simple practical adaptations for networks that may have broader applicability. For more general analysis, they may be significant, but for mitigation, they are near-essential. Additionally, single-sample assumptions are made in this theoretical introduction; a more thorough discussion is available in *App. B.1*. Overall, these ensure that many prior parameter corrections don't propagate their corrections too, as this would be highly nonlinear and extremely complicated/intractable to resolve. Additionally, propagation that terminates at the output of the affine layer offers simple solutions by avoiding highly variable and nonlinear activation functions, although these considerations [4] initially motivated this investigation.

Having established the need for such assumptions, one can now analytically calculate the effective correction to representations by computing the change in representations due to parameter adaptations. It is then imperative to determine whether this is equivalent to the mathematically ideal update of *Eqn. 2*. Computing such an effective representation correction is shown in *Eqn. 8* and assume for the same sample/batch, single-layer correction ( $x'_j = x_j$ ).

$$\begin{aligned} z'_i &= W'_{ij}x_j + b'_i \\ &= (W_{ij} - \eta g_i x_j) x_j + (b_i - \eta g_i) \\ &= z_i - \eta g_i (x_j x_j + 1) \\ &= z_i - \eta g_i (\|\vec{x}\|^2 + 1) \end{aligned} \quad (8)$$

---

<sup>2</sup>Simplified to remove covariant subscripts and contravariant superscripts, which are not needed here.

Here, one can see the effective correction to the representations.

Assuming  $\eta \rightarrow 0$ , and a reorganisation of *Eqn. 8* yields *Eqn. 9*. This can be thought of as the effective gradient, computed using a finite difference.

$$\frac{\Delta \mathcal{L}}{\Delta z_i} = -\frac{z'_i - z_i}{\eta} = g_i \left( \|\vec{x}\|^2 + 1 \right) \quad (9)$$

One can see that this is inequivalent to the mathematical ideal update of *Eqn. 2*, diverging through the term  $(\|\vec{x}\|^2 + 1)$ . This will be termed the “affine divergence” and can be summarised as *Eqn. 10* or the equality of *Eqn. 11*.

$$\frac{\Delta \mathcal{L}}{\Delta z_i} \neq \frac{\partial \mathcal{L}}{\partial z_i} \quad (10)$$

$$\boxed{\frac{\Delta \mathcal{L}}{\Delta z_i} = \frac{\partial \mathcal{L}}{\partial z_i} \left( \|\vec{x}\|^2 + 1 \right)} \quad (11)$$

Overall, this produces a sample-wise bias in the gradient step. In short, there is a disparity between the ideal and effective correction undertaken by representations, despite the agreement for parameters.

Notably, this derivation is for affine layers; it requires generalisation for other maps, such as convolution, which is discussed in *App. B.2*. For other maps, the divergence is qualitatively similar yet yields different solutions, such as a patchwise divergence for convolution, necessitating a ‘PatchNorm’ functional form.

## 2.2 Implications of the Affine Divergence

Despite gradient descent being implemented so that parameters take the optimal step to reduce the loss, it is observed that, to first order, single-layer approximation representations do not take the optimal step. Yet representations are a more direct quantity of interest, since they carry the sample-dependent information. They are also, in principle, more directly associated with the loss than any parameter they depend upon because, without parameter-loss regularisation, representations must always be subsequent to the parameters. Hence, representations downstream of parameters are directly closer to the loss and desired outputs in the computation graph, and classically constitute the quantities of interest, forward propagating the data-dependent information to the outputs.

Important questions to ask:

1. *What are the implications of the divergence? Considering whether it is theoretically pathological?*
2. *Should we prioritise the perfect step for the parameters at the expense of the representations?*
3. *Can we correct for this divergence, and can this be concurrently achieved for parameters and representations?*
4. *What are the consequences of such corrections?*
5. *Does empiricism validate the pathology of this divergence?*

This manuscript aims to develop each of these.

To begin, and in short, the implications of such a divergence are geometric. The effective update to representations is deflected from the direction of steepest descent. Such a perspective suggests that this may have a suboptimal or detrimental implication for learning.

One can see, from *Eqn. 11*, the presence of a squared magnitude of the samples scaling the gradient. These act as unintentional weightings to each’s respective gradient. Hence, inducing a sample-wise geometric inconsistency in the representation gradients, where large-magnitude samples produce disproportionately sized updates stepwise, and distorted, over-weighted updates batchwise. These result in a deflection from the ideal update trajectories and steepest descent, respectively.

In effect, a single-sampled update step would produce updates of various effective learning rates,  $\eta_{\text{eff.}} = \eta \left( \|\vec{x}\|^2 + 1 \right)$ , which may result in an overall deflection of optimisation trajectories. Similarly, if a gradient update is averaged over a batch, a few large samples will dominate the direction of the resultant representational gradient step relative to others, thereby skewing the direction of the update in their favour. Hence, in both scenarios, large-magnitude samples propagated through the affine layers may introduce a foundational bias in optimisation.

One may be considering that normalisation typically reduces such magnitudes, by altering activation distributions; however, this paper hypothesises that such a relation would be better framed in reverse: *Perhaps the success of normalisation is due to approximately correcting the representational update*. This consideration will then incidentally coincide with affine divergence solutions, which also appear normalisation-like.

Such a hypothesis is intriguing, since other normalisations [6, 7, 8] do not often provide a perfect correction to such terms, but only partial mitigation or a misscaled result. BatchNorm [6] may reduce  $\text{Var} \left( \|\vec{x}\|^2 + 1 \right) = \text{Var} \left( \|\vec{x}\|^2 \right)$  through confining the distribution of  $\vec{x}$ , but would not typically send it to identically zero. Generally, averaging over a

batch, as achieved through mini-/batched gradient descent, may similarly mitigate  $\text{Var}(\|\vec{x}\|^2 + 1)$ , adding a mechanistic explanation for its efficacy, but may not converge as nicely as  $\text{Var}(\|\vec{x}\|)$  due to the squared term presence. In both approaches, sample-wise fluctuations may persist and result in a mitigated, but still significant divergence. Both LayerNorm [7] and RMSNorm [8] operate differently; they do send  $\text{Var}(\|\vec{x}\|^2) \rightarrow 0$  but with significant caveats despite their sample-wise independence, including a non-ideal scaled representation corrections, a shift in the weight-bias responsibility in these corrections<sup>3</sup>, and complications of the geometry in backward and forward passes are discussed in subsequent sections.

Hence, overall, this affine divergence term may contribute to a fundamental mode in the success of current normalisations, by reducing the extreme over-weighting in large samples. However, if this is a fundamental causal mode, then the mitigation is only partial and may be fully corrected by the suggestions in the following section.

This enables one to produce a hypothesis to aid in determining the importance of such a term to the success of normalisation: *If this  $(\|\vec{x}\|^2 + 1)$  and its generalisations are responsible for normalisation's success, then a perfect correction would be expected to improve performance more than approximate corrections.* Hence, the test of this paper is to assess whether such a hypothesis holds, providing a good correlation with performance. This will be investigated through controlled ablation models, comparing different implementations. These models are kept purposefully straightforward to establish a clear result for mid-sized classification networks, where single-layer approximations remain within a valid regime without many prior layers compounding into substantial propagated corrections. This can later be extended in subsequent work.

The following section will derive several analytical and straightforward solutions to the divergence. Several of these are mathematically distinct from current implementations and, therefore, are especially interesting because they do not exhibit features typically attributed to normalisation's success. Using these in the comparative ablation-like approach provides insight into the mechanistic causes underlying normalisation's performance, allowing determination of whether it is the correction of the affine divergence or another reason that underlies empirical performance.

### 2.3 Deriving the Affine Corrections

The objective of this work is to explore the consequence when *Eqn. 12* holds true.

$$\frac{\Delta \mathcal{L}}{\Delta \vec{z}} = \frac{\partial \mathcal{L}}{\partial \vec{z}} \quad (12)$$

There are infinitely many ways to achieve such an equality; however, four forms will be primarily explored, yet should not be considered an exhaustive set of solutions.

Those solutions that produce exactly ideal parameters *and* representational gradient steps by altering the affine mapping will be termed “structural” corrections. These solutions affect both forward propagation and backpropagation non-trivially, including changing the parameter updates.

There are different forms for solutions, but they can be summarised as the functional form shown in *Eqn. 13*, with  $\alpha_{ij} \equiv \alpha_{ij}(\vec{x})$  and  $\beta_{ij} \equiv \beta_{ij}(\vec{x})$ . Different choices produce different families of solutions:  $\alpha_{ij} = \alpha_i$  or  $\alpha_{ij} = \alpha$  or  $\alpha_{ij} = \beta_{ij}$  etc. From this plethora of general functional forms, two primary corrections emerge, which shall be explored.

$$y_i = \alpha_{ij} W_{ij} x_j + \beta_{ij} b_i \quad (13)$$

The second general approach is to scale the gradient updates for parameters by introducing an amended learning rate. These will be termed “gradient-only” corrections. This still affects the forward propagation of activations in subsequent steps, but does not fundamentally change the affine maps present. This is the category under which natural gradients may be classified.

These classifications can then be further subdivided. For example, there are two structural map-updating procedures which will be focused on, given by either *Eqn. 14* or *Eqn. 15*<sup>4</sup>. These constitute a norm-like (*Eqn. 14*) and an affine-like (*Eqn. 15*) approach.

$$z_i = W_{ij} \left( \frac{x_j}{s} \right) + b_i \quad (14)$$

$$z_i = \frac{W_{ij} x_j + b_i}{s} \quad (15)$$

To then determine the effective representational corrections, the relevant updates must be propagated from parameters into representations, yielding *Eqn. 16*, corresponding to *Eqn. 14* (norm-like).

<sup>3</sup>Where ‘responsibility’ is described by the relative share of  $\Delta \mathbf{W}$ -to- $\Delta \vec{b}$  constituting  $\Delta \vec{z}$  in the equation  $\Delta \vec{z} = (\Delta \mathbf{W}) \vec{x} + (\Delta \vec{b})$ . If this is dominated by the bias, then the correction is primarily translationally acting as a global sample-independent offset. The relative responsibilities may be tuned due to this consideration.

<sup>4</sup>As indicated, any reweighting of these by  $\alpha \in \mathbb{R}$ ,  $\beta \in (-1, 1)$  also works, and is included in the infinite family of structural approaches. They result in a different balance between weights and bias contributions and differing proportions of updates. For  $z_i = \alpha W_{ij} \left( \frac{x_j}{s} \right) + \beta b_i$ ,  $s = \sqrt{\frac{\|\vec{x}\|^2 \alpha^2}{1 - \beta^2}}$  whilst  $z_i = \frac{\alpha W_{ij} x_j + \beta b_i}{s}$  yields  $s = \sqrt{\alpha^2 \|\vec{x}\|^2 + \beta^2}$ .

$$\begin{aligned}
z'_i &= W'_{ij} \left( \frac{x_j}{s} \right) + b'_i \\
&= \left( W_{ij} - \eta \frac{g_i x_j}{s} \right) x_j + (b_i - \eta g_i) \\
&= z_i - \eta g_i \left( \frac{x_j x_j}{s^2} + 1 \right) \Rightarrow s = \|\vec{x}\| \\
&= z_i - 2\eta g_i \rightarrow z_i - \eta' g_i
\end{aligned} \tag{16}$$

One can note that this produces a doubling of the effective learning rate. To make all results comparable, one should also halve the applied learning rate:  $\eta' = \frac{\eta}{2}$  as a hyperparameter. Both  $\eta$  and  $\eta'$  will be used in experiments to demonstrate this. Similarly, this half-factor can be absorbed into  $\alpha_{ij}$  and  $\beta_{ij}$  if desired, using that prior generalised formalism.

Overall, substituting the derived  $s$  in turn derives the ‘normaliser-like’ correction of *Eqn. 17*.

$$\boxed{\vec{z} = \mathbf{W} \left( \frac{\vec{x}}{\|\vec{x}\|} \right) + \vec{b} \quad (= \mathbf{W} \hat{x} + \vec{b})} \tag{17}$$

Similarly, one can compute the affine-like correction factor  $s$  for *Eqn. 15* as shown in *Eqn. 18*.

$$\begin{aligned}
z'_i &= \frac{W'_{ij} x_j + b'_i}{s} \\
&= \frac{1}{s} \left( \left( W_{ij} - \eta \frac{g_i x_j}{s} \right) x_j + \left( b_i - \eta \frac{g_i}{s} \right) \right) \\
&= z_i - \eta g_i \left( \frac{x_j x_j + 1}{s^2} \right) \Rightarrow s = \sqrt{\|\vec{x}\|^2 + 1} \\
&= z_i - \eta g_i
\end{aligned} \tag{18}$$

Substituting  $s$  derives the ‘affine correction’ of *Eqn. 19*.

$$\boxed{\vec{z}' = \frac{\mathbf{W} \vec{x} + \vec{b}}{\sqrt{\|\vec{x}\|^2 + 1}}} \tag{19}$$

In both cases, and when accounting for the effective learning rate, the solutions produce a new map which identically cancels the affine divergence. This means that the gradient steps for both parameters and representations are now mathematically ideal, and the effective update is in the direction of steepest descent as intended. The first solution, norm-like, is effectively a classical  $L_2$ -normalisation, similar to RMSNorm without a  $\sqrt{n}$  width factor. This implicates the affine divergence as being able to derive a normaliser from first principles. However, this second affine-like solution also remedies the affine divergence, yet is *not* a normaliser. If this latter form is successful and does not present as a classical normaliser, then it situates the affine divergence as an underlying mechanistic explanation for the success of such approaches. Hence, this second solution may be fundamentally significant to compare, since their joint success can then be attributed to the resolution of the affine divergence, as the second solution is a novel functional form and is wholly distinct in operation from a classical normaliser. Moreover, the affine-like correction has several notable, desirable qualities over classical normalisers, which are discussed in subsequent sections.

These solutions do differ substantially. One such difference can be used to subdivide both structural and gradient-only corrections as gestured. This is the proportionality of weight and bias updates with respect to the standard affine map, before and after the applied corrections. Where *Eqn. 18* keeps the proportions intact, just scaled down, whereas *Eqn. 16* selectively scales down the weights only, resulting in a disproportional effect. This dis/proportionality can be used as a further subdivision descriptor within each of the structural or gradient-only approaches. Thus, yielding four qualitatively distinct methods. Similarly, the  $1/\sqrt{n}$  factor from RMSNorm [8], acts as a disproportionate up-scaling on the weight’s gradients step by the factor  $\sqrt{n}$  compared to  $L_2$ -Norm relative to the bias. These proportionality are argued to place more onus on the weight’s ‘responsibility’ in the representational correction compared to bias, for RMSNorm, this emphasises weights as where the representational correction is realised. However, despite the dis/proportionality, both structural approaches still induce significant implications by substantially changing the forward pass and backward pass computations. This is discussed in the following section.

Finally, one can amend the gradient descent step *only* in various ways. Particularly, a global-layerwise corrected learning rate, as shown in *Eqn. 20* — keeping the proportions intact. However, due to the nature of autodiff, accumulating over samples upfront, this method is not implementable unless working with the full Jacobians directly, which is prohibitively expensive. Therefore, although theoretically plausible, in current approaches to backpropagation, it is not implementable, as it would require a sample-wise adjustment to the Jacobian, which is not accessible straightforwardly. A full rebuild of backpropagation using Jacobians could be undertaken in future work, but it is well outside standard practice.

$$\eta' = \frac{\eta}{\|\vec{x}\|^2 + 1} \tag{20}$$

Or one can apply it locally to just the weight matrices, and an overall halving of layerwise learning rate, as shown in *Eqn. 21* — producing a disproportionate change in gradients between weights and biases.

$$\begin{aligned}\eta'_{\mathbf{W}} &= \frac{\eta}{2 \|\vec{x}\|^2} \\ \eta'_b &= \frac{\eta}{2}\end{aligned}\tag{21}$$

Overall, the two structural solutions will be explored and can be categorised as ‘structural-disproportional’ (norm-like), ‘structural-proportional’ (affine-like), whilst the gradient-only approaches can be similarly termed ‘gradient-only-proportional’ and ‘gradient-only-disproportional’.

The batching of inputs complicates the approach and introduces a remaining ‘off-diagonal’ divergence. Consideration of such implications is important due to the pervasiveness of batched computations and their surprising relation to convolution. Such nuances are further discussed in *Apps. B.1* and *B.2*.

## 2.4 Discussions of the Affine Structural Corrections

As suggested, these corrections are not inconsequential. This is particularly relevant to the structural approach, which has both *direct* implications for the forward and backward passes; by contrast, the gradient-only type has direct implications only for the backward pass, and from this an indirect effect on the forward pass through the parameters of the same affine step.

First, the forward-pass implications will be discussed for the two structural forms: the affine-correction and the normalisation-like correction. The former produces an input-dependent scaling, acting somewhat as a soft bound on the output, as displayed in *Eqn. 22*.

$$\|\vec{z}\|^2 = \frac{\vec{x}^T \mathbf{W}^T \mathbf{W} \vec{x} + 2\vec{b}^T \mathbf{W} \vec{x} + \|\vec{b}\|^2}{\|\vec{x}\|^2 + 1}\tag{22}$$

However, crucially, it retains *all representational degrees of freedom*, but it does produce a nontrivial nonlinear remapping (discussed again in *App. A*).

The same cannot be said for the normalisation-like correction. This approach projects out the magnitude degree-of-freedom *irreversibly*. Consequently, there is a distinct change in the structure of the representations before and after the map. Information is lost, namely, the radial degree of freedom. This constitutes a map  $\mathbb{R}^n \rightarrow S^{n-1} \hookrightarrow \mathbb{R}^n$ , indicating it projects down to a unit-hypersphere manifold, before embedding this back into the  $\mathbb{R}^n$  space, obfuscating the loss. This is responsible for the classical (radial) scale invariance associated with such a normaliser-like approach. One may believe the additional parameter degrees of freedom compensate for this representational degree of freedom, but this is not so; they are fundamentally different quantities and cannot be substituted for one another.

Moreover, the normalisation-like approach has singular behaviour as  $\|\vec{x}\| \rightarrow 0$ , which isn’t smooth like isotropic activation functions [5, 4] — although  $\epsilon$  can help mitigate this (but does not resolve the latter exploding gradients argument).

However, the norm-like solution does represent a decomposable and therefore separate map from the typical affine layer. The decomposition is as if the affine layer precomposed with a normaliser, hence the association<sup>5</sup>.

Overall, this means that both structural solutions can act nonlinearly on representations when replacing the affine layer and used sequentially, although the affine approach crucially loses no representational degrees of freedom. This contrasts with the norm-like approach, which results in a loss of representational degrees of freedom and, hence, possibly non-redundant information. This does not appear favourable without a strong justification. Similar representational-degree-of-freedom losses are present for prior normalisers as well [6, 7, 8], as discussed in *App. A* and displayed in *Fig. 1*. The suppression/preservation of such degrees of freedom, over initially uncontrolled and absolute removal, is one arguably favourable characteristic of the affine-like solution over other normalisations.

<sup>5</sup>Here ‘normaliser’ is used non-standardly. In effect, the parameterised scaling and the overall map are treated as two separate, further-decomposable contributions for study. The latter becomes essentially indistinguishable from the notion of an activation function, blurring their distinction. This is because both typically apply a non-linear map when parameters are separated. This is discussed further in *App. A*.

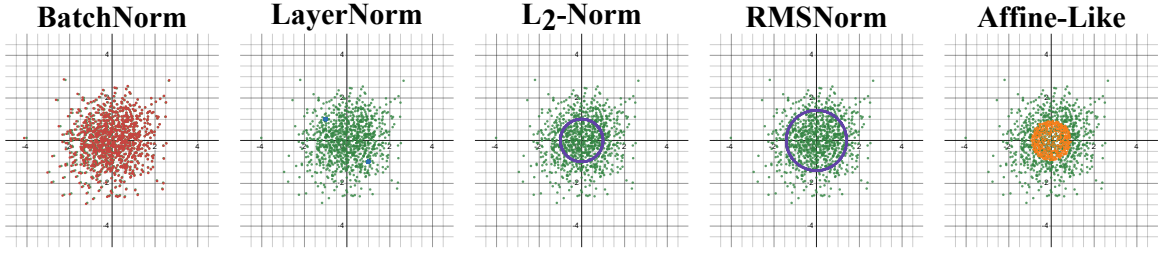


Figure 1: This plot displays the effect of various normalisers. This is depicted by drawing a thousand (green) input points drawn from a standard multivariate normal distribution in  $\mathbb{R}^2$ . Then, each plot depicts these initial input points in green and the resultant output distribution for each normaliser in a contrasting colour. The left demonstrates BatchNorm’s output in red, where statistics are computed over all 1000 input points and therefore produce little change in the output distribution, as the distribution is already standard-normal. Next is LayerNorm, which can be seen to collapse the entire distribution into two single blue clusters. This is because the LayerNorm map follows  $\mathbb{R}^n \rightarrow S^{n-2} \hookrightarrow \mathbb{R}^2$ . For  $n = 2$ , this results in  $S^0$ , which preserves only sign information. Typically, this would be a hypersphere orthogonal to  $\vec{1}$  in higher dimensions. Interestingly, the standard mean can be reweighted to *any* weighted mean, including one-hot, represented by  $\vec{x} - (\vec{x} \cdot \hat{n})\hat{n}$ , with geometrically minimal effect except for reorientating the hypersphere to be orthogonal to  $\hat{n}$  (unless algebraic anisotropic [5] function’s direction distinctions interact). This geometrically undermines the layer mean-statistic argument, which sometimes supports LayerNorm, since the one-hot weighting statistic is unaffected by layer width. This supports the transition from statistical interpretation to a geometrical one, which better aligns with the activation function decomposition suggested in App. A. Centre is  $L_2$ -norm, which projects the distribution into an  $S^{n-1}$  purple hypersphere, similarly to the next right, which is RMSNorm, which projects to a  $\sqrt{n}$  scaled hypersphere. Finally, a depiction of Affine-Like, for  $\mathbf{W} = \mathbf{I}_{n \times n}$  and  $\vec{b} = 0$ , shows how the distribution fills the volume of the hypersphere without projecting out the radial representation degree of freedom.

Furthermore, if the affine-like approach is empirically validated, then its success cannot be attributed to conventional gradient explanations. These partially helped motivate RMSNorm [8]. This departure can be seen in the comparisons between *Eqns.* 23 and 24 — which feature the gradient updates for the weights in the normalisation-like and affine-like correction, respectively.

$$\frac{\partial \mathcal{L}}{\partial \mathbf{W}} = \vec{g}\hat{x}^T \quad (23)$$

$$\frac{\partial \mathcal{L}}{\partial \mathbf{W}} = \frac{\vec{g}\vec{x}}{\sqrt{\|\vec{x}\|^2 + 1}} = \sqrt{\frac{\|\vec{x}\|^2}{\|\vec{x}\|^2 + 1}} \vec{g}\hat{x}^T \quad (24)$$

It can be seen that the affine-like approach does not make the weight update invariant to the magnitude of the input  $\vec{x}$ . Instead, it only limits to  $\vec{g}\hat{x}^T$  as  $\|\vec{x}\| \rightarrow \infty$ . An advantage of the affine-like over norm-like solutions is that it does not feature singular behaviour as  $\|\vec{x}\| \rightarrow 0$ , without the need for an additional  $\epsilon$  term violating the solution. Overall, for the affine-like map, the magnitude does modulate the weight update. Smaller magnitude inputs don’t adapt the weights as much, but larger updates all tend to update it to the same degree due to the bounding. Heuristically, this may also be desirable when considering the magnitude-direction hypothesis for representations. This is where direction encodes semantic meaning, and the magnitude represents the degree of stimulus presence. Hence, a small-magnitude input would indicate a lack of stimulus, suggesting it shouldn’t partake in a significant weight correction.

This generally contrasts with the normalisation-like approach, which is invariant to the magnitude of the input  $\vec{x}$  for weight updates. Therefore, if the affine-like change is empirically successful, then its success cannot be attributed to this magnitude invariance, only to the affine correction directly or possibly the upper-bounding. This provides another counterargument against attributing the success of normalisation to the invariance of parameters with respect to input magnitude, as discussed previously [8], and offers an alternative or additional explanation for the empirical success. The experiments in this paper find the affine correction often successful, greater or equally so than norm-like, suggesting that this weight-correction magnitude-invariance is not sufficient to explain the results.

In both cases, the affine divergence correction is invariant to  $\|\vec{x}\|$ , so perhaps instead it is the representational corrections’ invariance to the magnitude (and direction for single-samples) that could mechanistically additionally explain the success. Success in both cases would imply that the propagated effective update being unperturbed geometrically by  $\vec{x}$  is more likely causal, with the invariance in weight updates for norm-like being coincidental to this.

Also interesting is that these structural solutions to the affine divergence could both be considered isotropic-like in their effect, e.g.  $f(\|\vec{x}\|)\hat{x}$ . The natural emergence of such isotropic functions is interesting, and the affine-like correction on the vector  $\vec{x}$  is analytically reminiscent of Isotropic-tanh [5], when neglecting the bias terms. The comparison is shown in *Eqns.* 25 and 26, the non-bias contributions to the affine structural correction and isotropic-tanh directly. This could, in part, explain some of the success behind isotropic-tanh [5, 4]; however, it does not explain the effectiveness of isotropic functions more broadly. More generally, this novel ideal-effective alignment theory remains pertinent to isotropy as

previously suggested [4].

$$\mathbf{W} \underbrace{\sqrt{\frac{\|x\|^2}{\|x\|^2 + 1}}}_{\mathbf{f}(\|\vec{x}\|)\hat{x}} \hat{x} + \dots \quad (25)$$

$$\mathbf{W} \underbrace{\tanh(\|x\|)}_{\mathbf{f}(\|\vec{x}\|)\hat{x}} \hat{x} + \dots \quad (26)$$

Further, it is essential to characterise the effect that both the normalisation-like and affine-like structural corrections have on the backward pass. The standard affine layer backward pass with respect to input is shown in *Eqn. 26*, normalisation-like in *Eqn. 27* and affine-like in *Eqn. 28*.

$$\frac{\partial \mathcal{L}}{\partial x_n} = g_i W_{in} \quad (26)$$

$$\frac{\partial \mathcal{L}}{\partial x_n} = g_i \left( \frac{W_{in}}{\|\vec{x}\|} - \frac{W_{ij}x_j x_n}{\|\vec{x}\|^3} \right) \quad (27)$$

$$\frac{\partial \mathcal{L}}{\partial x_n} = g_i \left( \frac{W_{in}}{\sqrt{\|\vec{x}\|^2 + 1}} - \frac{y_i x_n}{\|\vec{x}\|^2 + 1} \right) \quad (28)$$

These equations demonstrate that backwards-propagating gradients acquire a dependence on the input  $\vec{x}$ , with implications for gradients in deeper models. This can reintroduce vanishing and exploding gradients through dependencies on  $\|\vec{x}\|$ . Crucially, however, the  $\vec{x}$ -dependent exploding possibility appears absent in *Eqn. 28*, as the denominator must be larger than 1 by definition. This would suggest a preferability of *Eqn. 28* over *Eqn. 27* by preventing such a  $\vec{x}$ -dependent growth in gradients. This complements the forward-pass advantage, which preserves all representational degrees of freedom, suggesting a general conceptual and mechanistic advantage of the affine-like correction.

The possibility of  $\vec{x}$ -dependent vanishing gradients may be partially mitigated by reintroducing parameterised scalings used jointly; this may partly explain their empirical necessity. Additionally, similar ideal-effective analyses may elucidate further relations, such as between residual steps and gradient magnitudes. However, this is complicated by the stated assumptions, as briefly discussed in *App. B.3*.

Furthermore, the implications of changing the proportionality of parameter updates may be significant. As stated, both the gradient-only and structural approaches can be further subdivided into proportional and disproportional approaches. These may change the onus of which form of parameter, such as weights or bias, contributes most significantly to the representational corrections. Changing these proportions is felt to be underdiscussed and has several potential ramifications. This could suggest that if the bias correction contributes a larger proportion of  $\vec{g}$  in the representational correction, then it is adapted more strongly, or is interpreted as more responsible, for the impact on representations. This may not be preferable since bias constitutes a simple global translation, rather than a position-dependent mapping.

Whether empirical performance is attributable to such changing proportions of the representation correction remains to be seen, but may be explored in terms of *Eqns. 29* and *30* — previously mentioned in a footnote, for  $\alpha \in \mathbb{R}$  and  $\beta \in (-1, 1)$ .

$$z_i = \alpha W_{ij} \left( \frac{x_j}{s} \right) + \beta b_i \quad (29)$$

$$z_i = \frac{\alpha W_{ij} x_j + \beta b_i}{s} \quad (30)$$

Overall, analyses of these various solutions will help determine whether the effective representational update agreeing with the mathematical ideal gradient step is responsible for the success of such methods. The comparison between norm-like and affine-like solutions also suggests that the affine-like correction is preferable, both conceptually and theoretically, to the normalisation-like approach. This is particularly due to the preservation of representational degrees-of-freedom in the forward pass, preventing  $\vec{x}$ -dependent gradient explosion in the backward pass, and naturally non-singular updates in the weight updates and forward pass without an  $\epsilon$  term, which subtly violates the solution. In addition, affine-like mappings lose the  $\|\vec{x}\|$ -scale invariance in the forward and backward passes, which is often attributed to normalisation success and functional-form motivation, respectively. Yet Affine-like's success in the comparative ablations undermines this as an essential characteristic, offering an alternative explanation based on affine divergence. This lack of scale-invariance, and other features, make this peculiar and novel second structural solution both interesting and discriminative for several classical explanations.

### 3 Results and Discussion

This section will overview a range of results from testing various normalisers and affine divergence solutions on networks consisting of sequential affine layers. Throughout this section, the results are for networks with affine layers of various

widths and depths, and activation functions. They are trained on CIFAR-10 classification with a consistent batch size of 32 for 100 epochs using a learning rate of 0.001. These hyperparameters were *not* optimised for each plot, but were selected as consistent, standard values to enable ablation comparisons. The plots show accuracy on the test set as a function of the number of training epochs, with the mean and standard *error* reported over 5 repeats.

The key system is given by “StandardAffine” in blue, which has no normaliser; “BatchNormAffine” in orange is affine layers precomposed with parameterless BatchNorm; “RMSNormAffine” in purple is affine layers precomposed with parameterless RMSNorm; “LayerNormAffine” in brown is affine layers precomposed with parameterless LayerNorm; “AffineCorrection” in red is affine-like structural correction presented in this paper; whilst both “L2NormAffineFull” and “L2NormAffineHalf” are the norm-like structural corrections of this paper using  $\eta' = \eta$  and  $\eta' = 0.5\eta$ , respectively.

Across *Figs.* 2, 3 and 4 plots, the title denotes the layerwise structure of the network, e.g. [3072, 32, 32, 3210], indicates three hidden layers of 32 neurons. Similarly, the layout is consistent, with the top rows of 1 hidden layer and the bottom rows of 3. Left-to-right columns always indicate plots for 16, 32, 64, and 128 width hidden layers.

The first plot, *Fig.* 2, demonstrates the performance of various normalisers and structural corrections applied to fully connected networks using Standard Tanh.

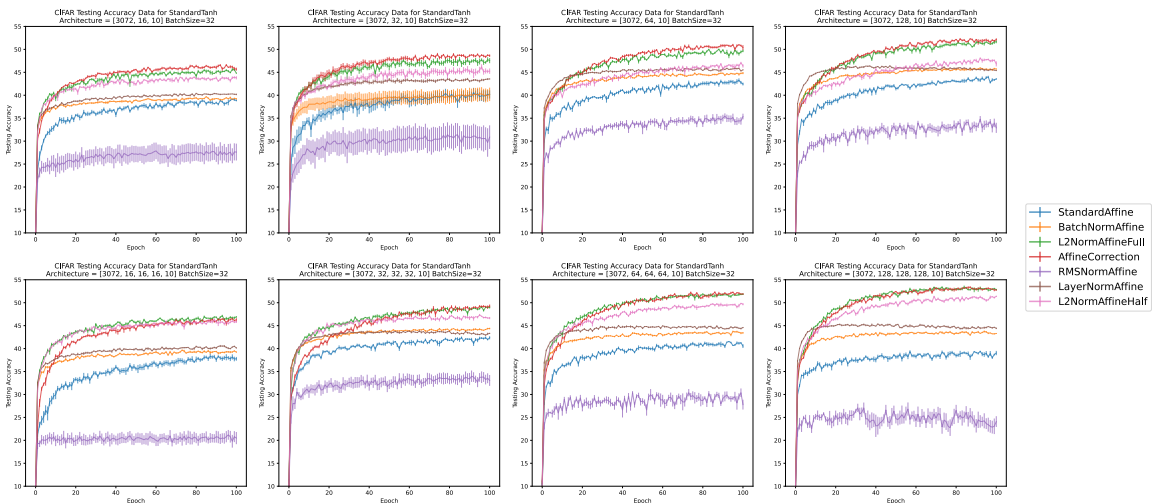


Figure 2: Displays the performance of Standard Tanh fully-connected sequential networks of various architectures. Immediately, one can observe that the affine-like correction (red) outperforms all other normalisers, except for 3-layer 16-width, where norm-like marginally outperforms it. Moreover, the affine-like and norm-like (half and full  $\eta$ ) performances are consistently substantially more performative than all other normalisers, having a wide margin between these normalisers and all others, especially for deeper networks. LayerNorm typically follows this, then BatchNorm, then no normaliser and then RMSNorm (showing the greatest and significant variability). It is notable that LayerNorm learns and stagnates the quickest in performance, whereas other normalisers take more time to build accuracy, with affine-like overtaking LayerNorm consistently around epoch 20. The surprising underperformance of RMSNorm may be due to both the architecture and the parameterless formulation.

The results from Standard Tanh indicate that, uniquely, the solutions which solve the Affine Divergence perform particularly strongly compared to all other normalisers. From these structural solutions, the affine-like formulation tends to perform notably better, as suggested by its favourable characteristics discussed in the previous section. The plot shown in *Fig.* 3 demonstrate this trend again for Leaky-ReLU.

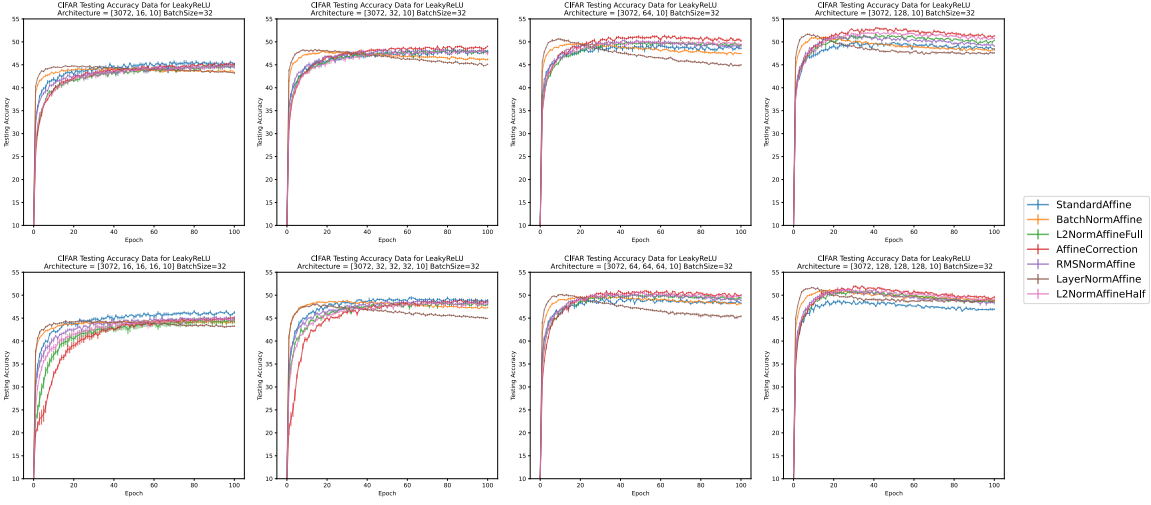


Figure 3: Displays the performance of Leaky-ReLU fully-connected sequential networks of various architectures. This plot is more nuanced: early learning is considerably faster across all normalisers, with a subsequent clear drop in performance for BatchNorm and LayerNorm only, before stagnation. This is sometimes observed in other normalisers as well, on longer timescales. As before, the affine-like correction typically performs best, particularly at larger widths and depths, where it exhibits a more distinct separation from all other normalisers. At very narrow networks,  $n = 16$ , no normaliser performs particularly well, followed by the affine-like correction. This is perhaps because the other normalisers remove representational degrees of freedom, which constitute a larger percentage of the representation volume in narrower-width networks. The clearest separation in performance is observed in the single hidden-layer  $n = 128$  plot, whereas the other plots are more overlapping. However, the standard error indicates that both affine-like and norm-like corrections consistently outperform alternatives.

As before, although the performances are more comparable, Leaky-ReLU also demonstrates a clear preference for the affine-like correction, with significantly better performance than alternative normalisers. Across various layer widths, these trends hold as shown in *Fig. 4*.

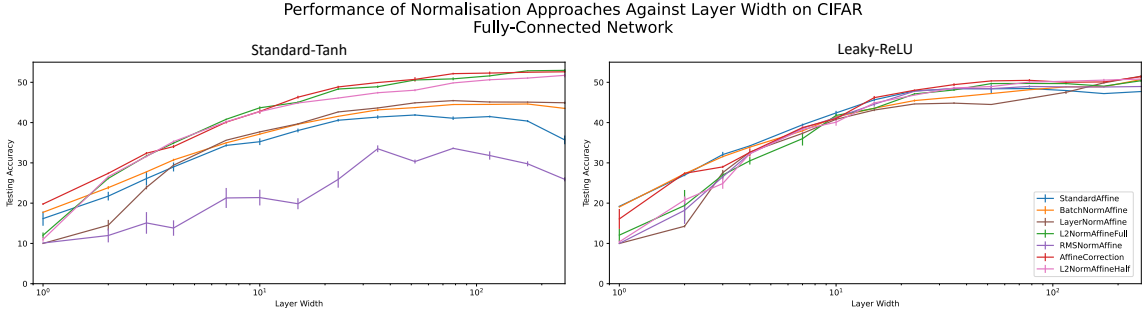


Figure 4: Plotted is performance against logarithmic layer-width for standard-tanh (left) and Leaky-ReLU (right), for layer widths ranging from 1 through 256. Training is otherwise identical to that in the other plots. Standard-tanh results show better performance separation, with the affine-like and norm-like structural solutions demonstrating significantly higher performance that grows with width, then begins to stagnate around a width of 128. The affine-like solution also performs notably better than alternatives even at a width of 1 neuron. Both no normaliser and RMSNorm reach a peak at  $n = 52$  and then decline again in performance. The ordering of normalisers follows from before: affine-like, then the two norm-like, then LayerNorm, BatchNorm, no normaliser and then RMSNorm. For Leaky-ReLU, the differences are slight, but Affine-like shows better performance at larger widths, while no normaliser outperforms at shallower widths.

Taken together, although these are smaller fully connected classification networks, the trend in results is clear. A tendency for affine-like structural solutions to outperform other normalisers, as hypothesised, is repeatedly observed, especially in deeper and wider network architectures. This is despite them not being a classical normaliser, as they do not feature scale invariance in either the backward or forward steps, fitting better into a geometric picture over a statistical interpretation, and preserving all representational degrees of freedom. Hence, such results, including the norm-like performances, are strongly suggestive that the affine divergence presents a novel theoretical mode through which normalisers may operate. Pursuing this led to both a classical normaliser and a non-normaliser-like solution, which consistently outperform alternatives, supporting the ideal-effective representational misalignment hypothesis and providing some counter-evidence to the scale-invariance theory.

Overall, this potentially positions the affine-like correction as a good and novel form of normalisers to be explored in larger architectures, *where the founding approximations continue to hold*. It also supports further investigation into the ideal-effective misalignment theory, generalising it across different architectures and approximations, and determining whether this yields broader performance benefits.

## 4 Conclusion

This work began with exploring the principle of a systematic mismatch between the ideal and effective updates taken by representations during optimisation. A theoretical divergence is demonstrated across fully-connected, convolutional, residual, and attention layers, suggesting the existence of multiple approaches to correct for the misalignment.

Of these, two primary structural corrections arose for the affine layer. One such solution closely resembled the functional form of normalisation, whilst the other was markedly different. Through this, a further explanatory mode for the empirical success of normalisation is developed and empirically substantiated. This is notable because the approach was entirely motivationally independent of normalisation, yet converged on this functional form incidentally during the exploration of the mismatch. Hence, it offers a direct *a priori* derivational justification for the use of normalisers, rather than a post-hoc explanation or empirical justification. Moreover, it provides another explanation: various prior normalisers may dampen this misalignment or over-scale updates, and their developmental chronology suggests that this mitigation is developing in a way that progressively approximates this solution.

Furthermore, by the conventional approach, the affine-like correction does not appear as a typical normaliser, and therefore its efficacy would not be evident. Nonetheless, it is theoretically derived as another distinct functional-form solution to the divergence. Furthermore, it empirically performs well, exceeding the performance of prior normalisers for affine layers across a range of affine architectures. Hence, supporting a new lens of understanding for the mechanisms of normalisation.

This is all reinforced by the secondary results reported in *App. B.1*, which predict a counterintuitive negative correlation between batch size and performance due to cross-sample interference, producing further ideal-effective misalignment. This is empirically validated in its respective results. This auxiliary prediction and verification strongly support the ideal-effective misalignment theory as a theoretical explanation for their success, rather than just an incidental or post-hoc explanation.

A secondary inference is that this may explain the success of isotropic functions in providing better effective-ideal alignment than anisotropic forms [4]; additionally, the affine-like solution appears to be functionally similar to isotropic-tanh [5]. This may also relate to the *App. A*, which encourages decomposing normalisers into two composable aspects: parameterised scalings and activation functions.

Although unorthodox, this situates modern normalisers [7, 8] as geometric operators above statistical ones in analyses. Geometrical implications include, but are not limited to, considering these normalisers as activation function maps that irreversibly reduce representational degrees of freedom. Similarly, Layernorm’s mean can be reweighted to be one-hot with no geometric consequences (except in the case of distinguished direction [9, 10, 4] interactions), indicating how statistics per-sample over the interdependent width-wise neurons are a nuanced matter. Unifying modern normalisers with activation functions can also recast functions such as RMSNorm as analogous to hyperspherical networks at intermediate layers. Hence, considering this normaliser–activation unification can undermine this tenuous but persistent categorical distinction in these often disparately considered operations. Therefore, their mechanistic efficacy may be better considered separately as these two maps, through which activation function theory could be unified.

The remaining appendices further develop this theory for various other maps, demonstrating the limits of the approximations that underpin the approach. A new form of convolution, with inbuilt normalisation, termed “PatchNorm”, is derived and developed, representing a new approach to normalisation that is not compositional but inseparable from convolution. Its discussion and results also elucidate the extent of approximations made for the theory. Additionally, both residual and attention divergences are outlined, with speculation that the lack of normalisation in attention may offer weak but circumstantial evidence for the theory overall.

Future work could also investigate the relation to the choice of optimiser, as these are likely non-trivial in effect, and the ramifications of rescaling by running statistics on *representation* updates could be further studied, such as element-wise rescaling by ADAM. These statistical estimates and rescalings do result in deflections of the *parameter*’s steepest-descent path for each batch, but their implications for the *representation* deflection are unclear, especially cumulatively over several steps. At least in the results obtained using ADAM [11], the proposed effective-ideal considerations continue to yield improvements.

Overall, the ideal-effective misalignment theory, incidentally a middle ground to the natural gradient approach under first-order, single-layer considerations, appears to independently provide a further mechanistic explanation of normalisers as a straightforward correction under these unique approximations. However, it also elucidates that normalisers are not the unique solution by predicting other beneficial mappings, such as the affine-like functional form, and the theory is predictive of several further phenomena, which are empirically validated. Hence, the normalisation-like map is derived, not assumed *a priori*, using *a priori* theory; a secondary non-normalisation affine-like map is derived as a solution and performs similarly or better, which itself cannot be explained by scale-invariance as it does not feature it. In conclusion, this suggests that the ideal-effective first-order misalignment theory may warrant further investigation of its scope and empirical practicality, and

that a philosophical shift in which corrections are prioritised may be a productive reconsideration more broadly.

## References

- [1] Shun-Ichi Amari. Natural gradient works efficiently in learning. *Neural computation*, 10(2):251–276, 1998.
- [2] Shun-ichi Amari, Ryo Karakida, and Masafumi Oizumi. Fisher information and natural gradient learning in random deep networks. In *The 22nd International Conference on Artificial Intelligence and Statistics*, pages 694–702. PMLR, 2019.
- [3] James Martens. New insights and perspectives on the natural gradient method. *Journal of Machine Learning Research*, 21(146):1–76, 2020.
- [4] George Bird. Emergence of quantised representations isolated to anisotropic functions, 2025. URL <https://arxiv.org/abs/2507.12070>.
- [5] George Bird. Isotropic deep learning: You should consider your (foundational) biases, October 2025. URL <https://doi.org/10.5281/zenodo.15476947>.
- [6] Sergey Ioffe and Christian Szegedy. Batch normalization: Accelerating deep network training by reducing internal covariate shift, 2015. URL <https://arxiv.org/abs/1502.03167>.
- [7] Jimmy Lei Ba, Jamie Ryan Kiros, and Geoffrey E. Hinton. Layer normalization, 2016. URL <https://arxiv.org/abs/1607.06450>.
- [8] Biao Zhang and Rico Sennrich. Root mean square layer normalization, 2019. URL <https://arxiv.org/abs/1910.07467>.
- [9] Nelson Elhage, Tristan Hume, Catherine Olsson, Nicholas Schiefer, Tom Henighan, Shauna Kravec, Zac Hatfield-Dodds, Robert Lasenby, Dawn Drain, Carol Chen, Roger Grosse, Sam McCandlish, Jared Kaplan, Dario Amodei, Martin Wattenberg, and Christopher Olah. Toy models of superposition, 2022. URL <https://arxiv.org/abs/2209.10652>.
- [10] George Bird. The spotlight resonance method: Resolving the alignment of embedded activations, 2025. URL <https://arxiv.org/abs/2505.13471>.
- [11] Diederik P. Kingma and Jimmy Ba. Adam: A method for stochastic optimization, 2017. URL <https://arxiv.org/abs/1412.6980>.

## A Separation of Parameterised Normalisers

In this work, often a ‘normalisation-like’ approach is discussed. However, these implementations are non-parameterised and not equivalent to typical normalisations implemented by libraries. This discussion will examine such choices, treating normalisers not as a single operation but as a two-step decomposition into a parameterised scaling and what amounts to a non-standard activation function.

Normalisations typically include two characteristic components: a parameterised scaling and some form of statistic-based or nonlinear mapping. For example, batch-norm standardises activations using the elementwise means and standard deviations over the batch, then scales and offsets using the parameterised  $\gamma$  and  $\beta$ .

The first step typically reduces the *representational* degrees-of-freedom (through the standardisation),  $\mathbb{R}^{bn} \rightarrow \mathbb{R}^{(b-1)n} \rightarrow S^{(b-2)n} \hookrightarrow \mathbb{R}^{bn}$ . Then the scaling introduces additional *parameter* degrees of freedom. This exchange of degrees-of-freedom from representational to parameterised *do not equate*, and can be reformulated as two individual and independent operations composed into one ‘normaliser’. Moreover, the parameterisation can, during the forward pass, be absorbed into existing affine parameters, although they diverge in gradient trajectories when separated.

Hence, these are two separate mappings, motivating separate treatment despite their composed usage. This work focuses on the non-parameterised step to draw equivalences with the affine correction. This is why BatchNorm/LayerNorm/RMSNorm are not parameterised in the methodology to enable fair comparison with such corrections.

For affine layers with a norm, the change in the number of representational degrees of freedom is as follows. One can see that the activation degrees of freedom are lost for all norms, but not for the affine correction.

- No norm:  $\mathbb{R}^{b \times n} \rightarrow \mathbb{R}^{b \times n}$ .
- Batch-Norm:  $\mathbb{R}^{b \times n} \rightarrow \mathbb{R}^{(b-1) \times n} \rightarrow (S^{b-2})^n \hookrightarrow \mathbb{R}^{b \times n}$ .
- Layer-Norm:  $\mathbb{R}^{b \times n} \rightarrow \mathbb{R}^{b \times (n-1)} \rightarrow (S^{n-2})^b \hookrightarrow \mathbb{R}^{b \times n}$ . One can see that, geometrically, this is BatchNorm operating on a different axis — much like a transposed version.
- RMS-Norm:  $\mathbb{R}^{b \times n} \rightarrow (S^{n-1})^b \hookrightarrow \mathbb{R}^{b \times n}$ .
- $L_2$ -Norm:  $\mathbb{R}^{b \times n} \rightarrow (S^{n-1})^b \hookrightarrow \mathbb{R}^{b \times n}$ .
- Affine Correction:  $\mathbb{R}^{b \times n} \rightarrow (S^{n-1} \times [0, 1])^b \hookrightarrow \mathbb{R}^{b \times n}$ , this does not suppress representational degrees-of-freedom, and acts more like performing a coordinate reparameterisation.

Secondly, the separation of these typically composed steps results in a loss of distinction between normaliser and activation functions, as both produce comparable mappings. One could reestablish such a distinction by normalisers reducing the representational degrees-of-freedom or that they use some form of statistic — although this is felt needless. Instead, their unification can be embraced, and this half of the normalisation step can be treated on equal footing to activation functions and their subsequent impact on representational geometry. Moreover, the distinction blurs further if considering parameterised activation functions.

This does not deny the empirical fact that combining these two aspects is successful, and they are usually considered as a whole. Instead, algebraically, we can consider normalisers to be a separable two-step process, which can be decomposed. One such step is largely algebraically indistinguishable from activation functions and pertinent to the affine divergence perspective. The former component is largely dropped in this discussion to allow a more comparable ablation test across differing approaches to determine the validity of this divergence hypothesis as a mechanistic route for the success of normalisers.

Hence, the current practice could be described as *normalisation + activation function*; however, it can perhaps be better reframed as *parameterised scaling + activation function + activation function*, then fusing the activation functions and merging the scaling with the affine transforms (although separate for differing gradient descent trajectories). By drawing such algebraic equivalences, the amended design approach can be reframed as the combination *parameterised scaling + activation function* and analysed in this manner moving forward.

If one does choose to also compose a *parameterised scaling*, then the affine divergence *must* be reconsidered, due to the addition of several new terms in the divergence. This is a higher order in the learning rate and is non-trivial to correct. This does not invalidate conclusions regarding normalisation, as the stated normaliser-like approaches still reduce the divergence, but may not identically cancel it.

If we consider the parameterised rescaling step as an additional affine layer, like those present in BatchNorm and LayerNorm, then when composed with the existing affine layer, it becomes the expression of *Eqn. 30*, with  $\tilde{x}$  indicating some preprocessing to  $\vec{x}$  — such as BatchNorm’s standardisation.

$$y_i = W_{ij} \underbrace{(\gamma_j \tilde{x}_j + \beta_j)}_{z_j} + b_i \quad (= W_{ij} \gamma_j \tilde{x}_j + W_{ij} \beta_j + b_i) \quad (30)$$

Implementing the gradient-descent step update yields *Eqn. 31*.

$$y'_i = (W_{ij} - \eta g_i \gamma_i z_j) (\gamma_j - \eta g_k W_{kj} \tilde{x}_j) \tilde{x}_j + (W_{ij} - \eta g_i \gamma_i z_j) (\beta_j - \eta g_k W_{kj}) + (b_i - \eta g_i) \quad (31)$$

This is an affine layer composed of another affine layer, with a diagonal scaling with respect to the standard basis. This two-layer approximation is much more complicated, as shown with the grouped  $\eta^2$  terms of *Eqn. 32*.

$$y'_i = y_i - \eta (g_i \gamma_j \gamma_i z_j \tilde{x}_j + g_k W_{kj} \tilde{x}_j W_{ij} \tilde{x}_j + g_i \beta_j \gamma_i z_j + g_k W_{kj} W_{ij} + g_i) + \eta^2 (g_k W_{kj} \tilde{x}_j g_i \gamma_i z_j \tilde{x}_j + g_k W_{kj} g_i \gamma_i z_j) \quad (32)$$

Overall, this additional diagonalised affine-scaling is separated from normalisation in this paper, predominantly because normalisation itself is two distinct algebraic maps that are composed and can be treated separately for greater clarity, and because the parameterised step confounds the divergence terms nontrivially. Upon separating the normaliser's composed scaling steps, it is argued that the distinction between the activation function and the normalisation becomes largely conventional rather than mathematically fundamental. It is therefore argued that most normalisers are algebraically more aligned with activation functions than any statistical operator, and should consequently be analysed as such. This motivates the explicit decomposition, in which only the statistical/nonlinear part is relevant to fixing the affine divergence, and the parameterised scaling introduces different divergences.

Generally, this unification between activation functions and normalisers is evident from *Fig. 5*, which displays similar results as before, but for classification networks *without* an activation function.

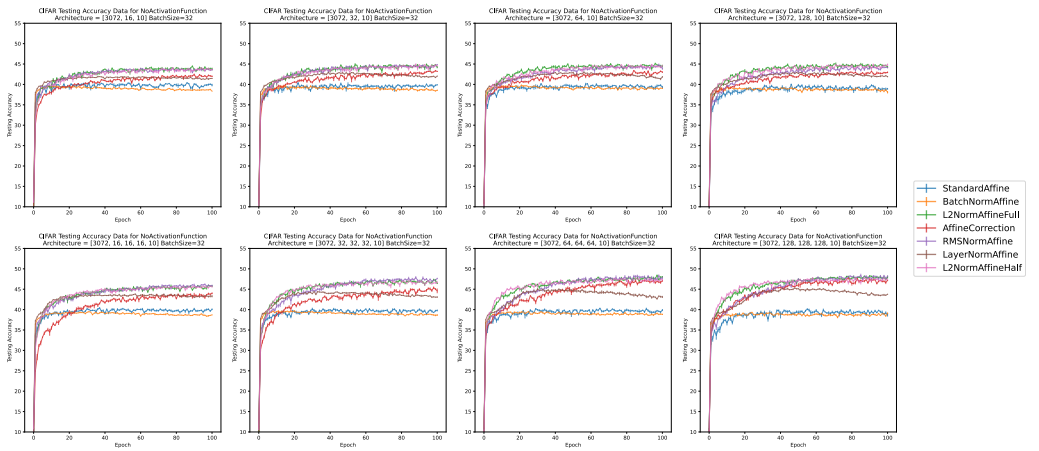


Figure 5: One can see across the results that both BatchNorm and no normaliser perform poorly, and similarly, this is because they are manifestly linear, so can achieve at most a linear fit. This is not the case for all other normalisers, which are nonlinear activation functions mathematically. There is a tendency for LayerNorm to be in the middle in performance, likely due to its additional losses in representational degrees of freedom. Affine-like follows this with some variability, then Norm-like, and RMS-like, which often perform similarly well. This may be because the latter two are more classical activation-function-like operations, which are composable with the affine layer, rather than being inseparable, as with the affine-like. Affine-like does enable folding of the activation distribution as can be seen from *Eqn. 22*.

Overall, this indicates that the normaliser decomposition into parameterised scalings and an activation function is a reasonable algebraic equivalence. Analysing normalisers in this decomposed approach may be more effective with its unification with modern activation function theory. Additionally, this decomposition has been utilised throughout this paper to investigate the nature of the nonlinear/statistical map only in relation to the affine divergence.

## B Divergence Generalisations

So far, this work has shown how the single-sample, first-order, affine divergence may be conceptually and empirically significant for deep learning. However, affine maps are far from the only form of mapping used in modern deep learning; moreover, batching is standard and so far underconsidered in this paper.

Hence, such considerations should be discussed in a more general picture. In this appendix, the implications for batched inputs, convolution, briefly residuals, and query-key attention are laid out. The derivations for convolution and batched-affine are surprisingly analogous, although different approximation choices may be selected with an apparent significant empirical consequence.

The (self-)attention approach suggests that such corrections may be intractable in the near term, or at least not a ‘cheap’ solution to implement. This may indicate why normalisation is not usually paired with a query-key attention step, perhaps because the divergence is not of the same form as that of affine layers; hence, adding a standard normaliser does not provide an advantage through correction.

### B.1 Batched Inputs

In this section, the batched-affine layer will be analysed, including the two proposed structural corrections, affine-like and norm-like, and how these interplay with the batched nature.

This indicates how batching is a more complicated consideration, and the resultant representational correction cannot often be perfectly ideal due to the parameter’s update being accumulated over several samples — thus providing an ‘averaged’-out representational correction which does not perfectly satisfy all samples simultaneously. This somewhat relates to the limits of linear maps.

To proceed, a short overview of the structural corrections are presented thus far.

$$y_i = W_{ij}x_j + b_i \Rightarrow y'_i = y_i - \eta g_i(x_j x_j + 1) \quad (33)$$

Two solutions are given in *Eqn. 34* and *35* for affine-like and norm-like structural corrections respectively (note  $t = s^{-1}$ ).

$$y_i = t(W_{ij}x_j + b_i) \Rightarrow y'_i = y_i - \eta g_i t^2 (x_j x_j + 1) \Rightarrow t = \frac{1}{\sqrt{x_j x_j + 1}} \quad (34)$$

$$y_i = tW_{ij}x_j + b_i \Rightarrow y'_i = y_i - \eta g_i (t^2 x_j x_j + 1) \Rightarrow t = \frac{1}{\sqrt{x_j x_j}} = \frac{1}{\|\vec{x}\|_2} \quad (35)$$

Now the batched generalisation can be explored, followed by what each of these approaches induces on the batch-wise picture.

A batched-affine map can be summarised as *Eqn. 36*, where  $b$  indexes the batch.

$$y_{bi} = W_{ij}x_{bj} + 1_b b_i \quad (36)$$

The respective gradients are given by *Eqns. 37*

$$\frac{\partial \mathcal{L}}{\partial y_{nm}} = g_{nm} \quad \frac{\partial \mathcal{L}}{\partial W_{nm}} = g_{kn}x_{km} \quad \frac{\partial \mathcal{L}}{\partial b_n} = g_{kn}1_k \quad (37)$$

One can see that there is now a gradient matrix, rather than a vector, with respect to  $y_{nm}$ . For representations, this batchwise index is preserved, whereas for both  $W_{nm}$  and  $b_n$ , a contraction automatically accumulates the batchwise gradients, according to the accumulation specified by  $\mathcal{L}$ , such that the batch is no longer expressed in their gradient. This is because the activations carry sample-specific information; in contrast, parameters are reused across all batches. A perhaps unusual restatement of this is that there is weight sharing across samples.

Additionally, this loss-induced accumulation of gradients over samples for the parameters is typically linear, e.g. a mean. This is a subtly different consideration from the clear linear contractions in the backpropagation step.

Substituting these in as a gradient descent step and propagating to a representational update yields *Eqn. 38*.

$$\begin{aligned} y'_{bi} &= y_{bi} - \eta (g_{ki}x_{kj}x_{bj} + g_{ki}1_b 1_k) \\ y'_{bi} &= y_{bi} - \eta g_{ki} \underbrace{(x_{kj}x_{bj} + 1_b 1_k)}_{= \mathbf{M}_{bk}} \\ y'_{bi} &= y_{bi} - \eta \mathbf{M}_{bk} g_{ki} \end{aligned} \quad (38)$$

We can observe here a more complicated affine divergence  $g_{bi} \neq \mathbf{M}_{bk} g_{ki}$ , unless a scaled identity matrix forms:  $\mathbf{M}_{bk} = \mathbf{I}_{bk} (= \delta_{bk})$ , requiring differing samples to all simultaneously have an inner product of  $-1$ . However, in general, a gram-like matrix divergence arises batchwise. This causes a sample-wise linear mixing of the gradient  $\mathbf{M}_{bk} g_{ki}$ , which is expected given the parameter updates with respect to the batch-accumulated gradients.

An interpretation is that the representation correction is somewhat (weighted-) averaged over the batch. This also means that not all steps are often simultaneously ideal. Without structural corrections, this weighted sum may be far from the ideal step for representations, e.g.  $g_{bi}$ .

One could experiment with a correction factor, e.g.  $y_{bi} = t_{kb} (W_{ij}x_{kj} + 1_{kb})$ , but this requires a matrix (pseudo-)inverse square-root matrix, which is computationally very expensive. Pseudo-inversion is especially needed when the index length of  $j$  is not equal to that of  $b$ , or when there is rank deficiency. Furthermore, this would also mix batch information non-trivially and likely undesirably for most forward-pass applications.

Instead, we can begin by investigating the two structural corrections, which will elucidate their implications on the batchwise picture. The two approaches yield corrections *Eqns.* 39 and 40 for affine-like and norm-like, respectively.

$$y'_{bi} = y_{bi} - \eta g_{ki} \frac{x_{kj}x_{bj} + 1_{bk}}{s_b s_k} \quad : \quad s_n = \frac{1}{\sqrt{x_{nm}x_{nm} + 1_n}} \quad (39)$$

$$y'_{bi} = y_{bi} - \eta g_{ki} \left( \frac{x_{kj}x_{bj}}{s_b s_k} + 1_{bk} \right) = y_{bi} - \eta g_{ki} (\hat{x}_{kj}\hat{x}_{bj} + 1_{bk}) \quad : \quad s_n = \frac{1}{\sqrt{x_{nm}x_{nm}}} \quad (40)$$

Two immediate conclusions are that the diagonal terms dominate due to these two corrections. This is conceptually notated in *Eqn.* 41, notatiomally  $\mathbf{N}_{bk} = (1_{bk} - \delta_{bk}) \mathbf{M}_{bk}$  equally  $\mathbf{M}_{bk} = \delta_{bk} + \mathbf{N}_{bk}$ , which preserves only the off-diagonal entries of  $\mathbf{M}_{bk}$ . Moving forward  $\mathfrak{D}_{ij} = (1_{bk} - \delta_{bk})$  will indicate the off-diagonal ones, e.g.  $\mathfrak{D}_{ij} + \delta_{ij} = 1_{ij}$

$$y'_{bi} = y_{bi} - \underbrace{\eta' g_{bi}}_{\text{Ideal}} - \underbrace{\eta' \mathbf{N}_{bk} g_{bk}}_{\text{Effective Interference}} \approx y_{bi} - \eta' g_{bi} \quad \text{since} \quad |\mathbf{N}_{bk}| \leq 1_{bk} \quad (41)$$

Therefore, the change in  $y_{bi}$  is most significantly *weighted* towards  $g_{bi}$ , and therefore, when assuming i.i.d. samples and with similar magnitude  $g_{bi}$ , will tend to dominate the correction for the sample. This is the desired ideal update step, encouraged by the two structural corrections. This is followed by some smaller magnitude of ‘interference’ corrections  $\mathbf{N}'_{bk} g_{ki}$ , due to other sample gradients in the off-diagonal terms. Secondly, the persistent  $1_{bk}$  generally adds a weighting to off-diagonal terms unless  $\hat{x}_{kj}\hat{x}_{bj} = -1$ . Hence, these are all positively weighted sums of  $g_{ki}$ .

Denoted more directly, *Eqns.* 42 and 43 demonstrate the diagonal and off-diagonal decomposition explicitly.

$$y'_{bi} = y_{bi} - \eta g_{bi} - \eta g_{ki} \left( \mathfrak{D}_{bk} \frac{x_{kj}x_{bj} + 1_{bk}}{\sqrt{x_{bm}x_{bm} + 1_b} \sqrt{x_{km}x_{km} + 1_k}} \right) \quad (42)$$

$$y'_{bi} = y_{bi} - 2\eta g_{bi} - \eta g_{ki} (\mathfrak{D}_{bk} (\hat{x}_{kj}\hat{x}_{bj} + 1_{bk})) \quad (43)$$

In both cases, the leading weighted correction then becomes  $\propto g_{bi}$  as desired, approximating the affine correction. Other terms then produce slight further geometric corrections, weighted by this off-diagonal sample-mixing matrix. If a particularly large  $g_{ki}$  is still present, then this may adversely affect the result if it overpowers the  $\mathbf{N}_{kb}$  suppression, leading to a poorer performing sample before and after update, but generally  $g_{bi}$  should probabilistically lead due to the favoured weighting.

One could explore bounding  $g$ ’s magnitudes, e.g. norm clipping, such as to suppress this eventuality. Exploring whether this generally aids performance by making all samples contribute an equal magnitude of correction, similar to suppressing  $\|\vec{x}\|^2 + 1$  throughout this work, may be an interesting direction that also links this paper’s exposition to norm-clipping techniques. Overall, as a heuristic, we may expect that these structural corrections produce more ideal gradient steps for representations and contribute an overall benefit samplewise, at least if these smaller off-diagonal steps are not drastically damaging to the overall correction.

Most importantly, the dominant diagonal ideal correction with sample-mixing interference can be interpreted to provide another falsifiable auxiliary hypothesis for this theory.

As the batch size increases, there is no fixed norm for the contribution of interfering terms; therefore, with a greater number of samples, we would expect greater interference to occur. This results in a geometric deflection away from the ‘ideal’ representational update per sample. As a direct consequence, one could predict that with respect to this theory, a greater number of samples should directly *degrade* the efficacy of the structural corrections.

This would not be the case for other normalisers, which may function differently in the representation alignment picture. For functions, such as BatchNorm, we may expect that an increasing number of samples would better produce better statistics (conventional picture) or better approximate damping of the  $\text{Var} \|\vec{x}\|^2$  (ideal misalignment picture), reducing the impact of individual detrimental fluctuations over the accumulated batch, potentially improving performance. A similar argument can be made for no normaliser, where batches stabilise gradient updates when accumulated (to some degree, this may also counteract the negative correlation hypothesised from the theory).

This simple hypothesis can be trivially tested by comparing performance across batch sizes for various normalisers, as shown in *Fig.* 6 for standard-tanh and *Fig.* 7 for Leaky-ReLU. These are for 2 hidden layers with a width 32 for classification on CIFAR-10.

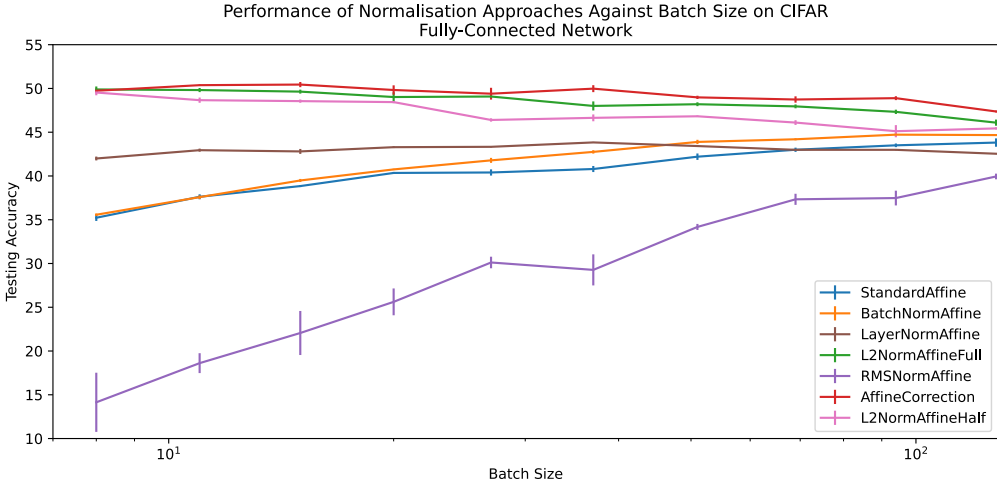


Figure 6: Displays the CIFAR10 test set accuracy for a batched-affine classification network using standard tanh, against differing batch sizes ranging from 8 to 128 samples per batch, over 100 epochs. One can see that two structural corrections, “ $L_2$ -Norms” (half,  $\eta/2$  and full,  $\eta$  — all other experiments using  $\eta = 0.001$ ) and “Affine Correction”, negatively correlate final accuracy with batchsize. This contrasts with LayerNorm, which is approximately constant, and BatchNorm, Standard Affine (e.g., no normalisation), and RMSNorm, which all positively correlate. Across all cases, the three structural corrections outperform all other approaches. These results are also for de-parameterised normalisers consistent with the discussion in *App. A*; which accounts for any seemingly non-standard normalisation results (i.e. low performance of RMSNorm). Error bars indicate standard error, equivalent to the error on the mean statistic.

One can see immediately that the two structural corrections have a relation where increasing batch size negatively correlates with performance for batched-affine layers — this is not the case for other prior normalisers.

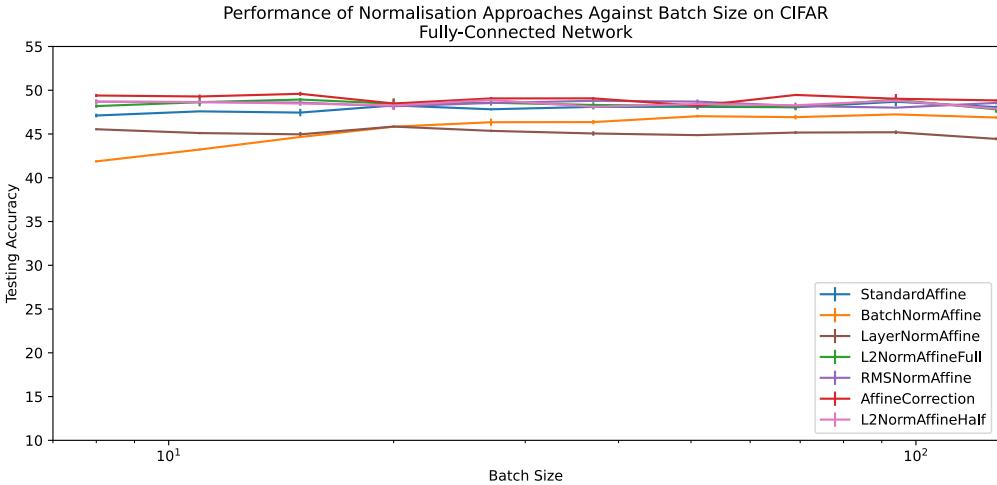


Figure 7: Displays the CIFAR-10 test set accuracy for a batched-affine classification network using Leaky-ReLU, against differing batch sizes ranging from 8 to 128 samples per batch, over 100 epochs. Mean and standard error are shown. Similar to previous results, these performances are much more comparable and difficult to separate. Across all samples, the affine correction is the best-performing and exhibits a slight negative correlation, tabulated below.

The correlations are tabulated in *Tab. 1*.

Across all cases, the affine-like correction outperforms other normalisers and is consistent with prior results. Moreover, all affine-like slopes,  $L_2$ -Norm (norm-like correction) at half  $\eta$  have a negative correlation with batch size, whilst  $L_2$ -norm at full  $\eta$  has a negative slope for standard-tanh, but a slightly positive, near flat slope, for Leaky-ReLU, but with a proportionally very larger error, reducing any significance to this. Across standard tanh results, these are all significant, with a small relative error compared to the negative slope. Similarly, for Leaky-ReLU, although the affine correction has a larger error. Generally, for Leaky-ReLU, all slopes are significantly smaller due to the more comparable results. LayerNorm also exhibits a negative slope, but the theory does not make *any* predictions regarding LayerNorm, so minimal interpretation is possible — similar for RMSNorm’s negative slope for Leaky-ReLU.

Normaliser	Standard Tanh		Leaky ReLU	
	Avg. Acc.	Slope	Avg. Acc.	Slope
Standard Affine	$38.35 \pm 0.50$	$(5.80 \pm 1.17) \times 10^{-2}$	$47.56 \pm 0.07$	$(5.51 \pm 2.83) \times 10^{-3}$
BatchNorm + Affine	$39.08 \pm 0.87$	$(5.04 \pm 1.21) \times 10^{-2}$	$45.54 \pm 0.67$	$(3.56 \pm 0.86) \times 10^{-2}$
LayerNorm + Affine	$43.72 \pm 0.21$	$(-8.77 \pm 2.45) \times 10^{-3}$	$45.59 \pm 0.15$	$(-8.58 \pm 3.00) \times 10^{-3}$
RMSNorm + Affine	$27.31 \pm 1.87$	$(1.05 \pm 0.210) \times 10^{-1}$	$49.15 \pm 0.21$	$(-5.38 \pm 2.45) \times 10^{-3}$
$L_2$ -Norm + Affine ( $\eta$ )	$49.93 \pm 0.10$	$(-2.98 \pm 0.20) \times 10^{-2}$	$48.50 \pm 0.22$	$(7.11 \pm 37.42) \times 10^{-4}$
$L_2$ -Norm + Affine ( $\eta/2$ )	$48.42 \pm 0.35$	$(-2.58 \pm 0.53) \times 10^{-2}$	$48.74 \pm 0.04$	$(-6.19 \pm 1.00) \times 10^{-3}$
Affine-Like Correction	<b><math>50.56 \pm 0.13</math></b>	<b><math>(-2.45 \pm 0.17) \times 10^{-2}</math></b>	<b><math>49.80 \pm 0.23</math></b>	<b><math>(-4.19 \pm 3.32) \times 10^{-3}</math></b>

Table 1: Displays the average accuracy of networks on CIFAR-10 taken across various batch sizes, alongside the slope of accuracy against batch size for these networks. Blue indicates negative slopes, and emboldening indicates the highest accuracy. These are taken by fitting a linear regression to the data points.

Overall, this appears to strongly support the auxiliary hypothesis, showing a surprising result: greater batch sizes tend to negatively correlate with structural corrections, which may be counterintuitive and classically surprising.

The RMSNorm (and to similar extent LayerNorm), are surprising as their representation updates follow a similar rescaling,  $y'_{bi} - y_{bi} = -\eta g_{ki} (n \hat{x}'_{kj} \hat{x}'_{bj} + 1_{kb})$ , with  $\hat{x}'_{bj} = \vec{x}_{bj} - \hat{1}_{bk} \vec{x}_{bk} \hat{1}_{bj}$  for LayerNorm only, and RMSNorm  $\hat{x}'_{bj} = \vec{x}_{bj}$ , where  $\vec{x} \in \mathbb{R}^{B \times n}$ . This  $n (= 32)$  weighting in the correction would imply an additional onus on the weights for providing the representational correction, seen especially if  $\eta \rightarrow \eta/(n+1)$ . Effectively, this a redistribution of responsibility for the representation update between parameters. The summation of weighted  $g_{ki}$  is more complicated in such a picture, with the presence of potentially large negative weightings, although with a remaining dominant diagonal and a relatively much larger amplification of cross-sampling coupling. LayerNorm also shows a negative correlation, but the sum over positive and negative off-diagonal terms may themselves also interfere. Hence, it is presently unclear how to determine a relation with batch size.

Perhaps, with a greater batch size, more positive and negative contributions could also tend to cancel out (if  $g_{ki}$  are similar across  $k$ , which may be more likely at larger batch sizes). In contrast, in positive-only  $L_2$ , they'd grow in effect. Additionally, in larger samples, the various  $\vec{x}$  may spread more evenly across the available volume, leading to more effective cancellation of both positive and negative cross-terms.

A shift in parameter responsibility may also be impactful. In any case, determining such an effect for both LayerNorm and RMSNorm is complicated, and not directly hypothesised as a result of the ideal-effective misalignment at this stage. Hence, their results should not be used to in/validate the theory, since the prediction of decreasing performance pertains only to the  $L_2$ -norm, which is empirically validated. Further research may better elucidate RMSNorm and LayerNorm's dependence. Nevertheless, the batchwise mixing term  $M_{bk}$  is present only in the *representation*-propagated corrections and downstream, suggesting it is implicated in these observations to some degree.

BatchNorm's trend, as mentioned, appears consistent with the damping/removal of  $\text{Var} \|\vec{x}\|^2$  by confining the distribution via batch statistics, and also convergence by batch averaging. Hence, in the representation update picture, BatchNorm appears not to improve performance by identically cancelling these sample-dependent terms, but rather by damping  $\text{Var} \|\vec{x}\|^2$  to reduce the ideal-effective divergence, resulting in a positive batchsize-performance correlation. Other classical modes for BatchNorm's success may also be pertinent.

Overall, the results support that the cumulative interference from off-diagonal terms does grow with batch size, impacting the overall accuracy. This appears to produce the surprising and non-standard negative correlation with batch size. These considerations aid in isolating this mode as causal. This is an entirely distinct secondary falsifiable hypothesis that further and strongly supports the ideal-effective misalignment theory, not merely as an incidental but *a* predictive mechanistic explanation of normalisation's empirical success. This, in addition to evidence that the affine-like correction is successful despite not being a typical normaliser, suggests that this divergence theory may be significant. Such a result at least appears interesting with respect to the role of the affine divergence in the empirical success of normalisation, and it is suggested that this warrants further consideration.

### B.1.1 The Sample Individuality Decision

The two structural corrections are mathematically shown to weight the sample-wise representational correction towards each sample's ideal gradient step. From an individual sample perspective, this appears beneficial. Yet, from the batched perspective, this remains non-ideal with the possibility of further improvement — although to implement this is computationally prohibitive and conceptually undesirable to create general interdependency between samples on the forward pass<sup>6</sup>.

<sup>6</sup>This interdependence of samples is substantively different from the estimated batchwise statistics stored and used in BatchNorm at inference, instead in this picture, such running estimates are not possible as a sample-dependent coupling is needed to be computed every time for the current specific samples.

Hence, these decisions regarding structural corrections entail an implicit prioritisation of sample individuality. The choice is made not to implement batchwise coupling, which might *in principle* yield a lower aggregate loss in the affine-divergence picture; instead, each sample is engineered such that the leading term is its ideal gradient, which may be most important for individually reducing that sample’s overall loss but not the ensemble due to the residual batch-divergence.

It suggests that these updates are still effective at reducing the loss individually; the overall batch loss is then straightforward to accumulate from these individual samples: a (linear) mean combination.

Consequently, the gradient  $g_{bi}$  has a sort of implicit linearity in  $b$ , despite its strong non-linearity in  $i$ ’s relations (e.g. the only cross terms in  $b$  arise linearly in the loss-step, this is not so for  $i$ ). This makes each sample’s drop in loss correspond to a decline in the batch loss due to the straightforward linear combination of individual samples in the loss (neglecting spurious increases samplewise from  $\mathfrak{D}_{kb} \mathbf{M}_{kb} g_{ki}$ ). This is an implicit choice of sample-independence made as an approximation, and it is seemingly heuristically favourable in the batch picture.

This consideration does not apply if all samples are non-linearly mixed in the forward pass to yield a final outcome. Despite the superficial linear contraction of  $g_{bi}$ , the evaluation of  $g_{bi}$  becomes very non-linear with respect to the batched-index of  $x_{bi}$ , and such a motivation of sample-wise independent prioritisation no longer holds. In this case, the presence of non-ideal off-diagonal terms may be much more damaging overall, even if it offers *some* improvement upon no normalisation, although even this may be doubtful.

This is conceptually significant. As in the subsequent section, it will be demonstrated, perhaps surprisingly, that the batched-affine and convolutional are structurally identical in the ideal-effective gradient picture, where patches act like the batched index. In short, batched affine layers are much like convolving the network sample-wise. Despite the unexpected parallel, these patches are not independent and are not accumulated linearly in the loss, as individual samples are. Hence, despite the structurally identical divergence, the partial structural corrections do not offer a straightforward solution.

The following subsection discusses this convolutional case and why such structural corrections are not clear, despite superficially being identical to the batched divergence.

## B.2 Convolutional Divergence

Qualitatively, the divergence occurs similarly for convolutional layers, but implementation-wise, the correction diverges strongly from current practice, suggesting a Patch-wise consideration over layer/group/batch-wise.

Potential solutions to a convolutional divergence are again numerous; yet, several will be showcased. Particularly, a novel approach to the application of normalisation in convolution is presented, to be termed “*PatchNorm*”, which, unlike the pre/post-composition of normalisation usually accompanying convolution, PatchNorm is an intrinsic change to the convolution procedure itself.

First, a parallel will be drawn with the discussion of *App. B.1*, requiring reformulating the typical convolution expression shown in *Eqn. 44*.

$$y_{ijd} = W_{abcd} x_{(i-a)(j-b)c} + b_d \quad (44)$$

Equivalently in function, one can ‘unroll’ convolution to express ‘patches’ as an index matrix  $x_{ijc} \rightarrow \tilde{x}_{pe}$ , where  $p$  indexes each patch per sample, and  $e$  indexes the dimensions per patch. Notably,  $\tilde{x}$  contains many repeated instances of the original  $x_{ijc}$  elements due to the patchwise unfolding. Overall, with corresponding reshaping of  $W$ , convolution becomes equivalent to *Eqn. 45*.

$$\tilde{y}_{pd} = 1_p W_{ed} \tilde{x}_{pe} + 1_p b_d \quad (45)$$

Comparing this to *Eqn. 36* one can see that these two operations are structurally identical in terms of matrix algebra (differing only in the  $1_p$ , which is made explicit in convolution to indicate the patchwise broadcasted weights, it is implicit in *Eqn. 36*). Thus, the convolutional divergence is shown in *Eqn. 46*.

$$\begin{aligned} \tilde{y}'_{bi} &= \tilde{y}_{bi} - \eta (1_p 1_k g_{kd} \tilde{x}_{ke} \tilde{x}_{pe} + g_{kn} 1_k 1_p) \\ \tilde{y}'_{bi} &= \tilde{y}_{bi} - \eta g_{kd} (\tilde{x}_{ke} \tilde{x}_{pe} + 1_{kp}) \end{aligned} \quad (46)$$

Hence, the divergence is also structurally *identical* to the case for batched affine. However, notable crossover in patched inputs does occur with instances of repeated value in  $\tilde{x}$  induced by the unrolling — this is unlike the batched case *in general*. Similarly, this equation could be expressed with an additional batched index  $b$ , but structurally does not cause a different divergence as it can be equally absorbed into a flattening and reindexing of  $p$  — so is notationally neglected for simplicity (although differing by instead inheriting the single-sample assumptions of *App. B.1*).

Of course, one could still implement the same structural corrections for empirical confirmation, yielding two new forms of deep learning map “*PatchNorm*” for Patch-Normalised-Convolution. These new ‘normalisers’ are inseparable from convolution, in contrast to typical normalisation functional forms that can be used in composition. Hence, two primary forms of PatchNorm can be introduced, in complete analogy to the affine corrections, *Eqns. 47* and *48*, analogous to affine-like and norm-like approaches respectively.

$$\tilde{y}_{pd} = t_p (1_p W_{ed} \tilde{x}_{pe} + 1_p b_d) \quad \Rightarrow \quad t_b = \frac{1}{\sqrt{\tilde{x}_{ba} \tilde{x}_{ba} + 1}} \quad (47)$$

$$\tilde{y}_{pd} = (t_p W_{ed} \tilde{x}_{pe} + 1_p b_d) \Rightarrow t_b = \frac{1}{\sqrt{\tilde{x}_{ba} \tilde{x}_{ba}}} \quad (48)$$

Yet, for convolution, the underlying approximations used to justify these single-sample corrections in batched cases are fundamentally broken by the non-linear mixing of individual patches to produce the output. This means that the approximations are not justified for convolution.

Therefore, despite the identical arithmetic to that of batched affine, the breakdown of a core approximation makes it unclear whether these implementations are supported. There are also strong inductive-bias arguments against perfectly correcting for the divergence, as it interferes with locality.

Overall, despite their structural appearance, patches are not comparable to samples in nature. Treating batched samples independently, neglecting batch-coupling corrections, is considered a defensible approximation and is consistent with how the loss aggregates individual samples linearly. They are treated as individually and equally important in correction, each acquiring a  $1/n$  weight in the loss. On average, individually aligning one sample’s representational update is expected to reduce that sample’s loss more than optimal parameter steps alone. This individual reduction is then linearly impactful on the overall batch’s loss as discussed.

Such a case for convolution is not clear. Patches do not contribute independently or linearly to the loss; they are repeatedly non-linearly combined to yield the final loss for a single sample. Moreover, the  $N - 1$  cross-sample interference terms for single-sample approximation, treated as more negligible, become the quadratically greater  $N(N - 1)$  cross-patch interference terms for a single sample patchwise — all contributing to the same single sample loss. Hence, it is likely that these are not negligible per sample but considerable in their cumulative effect, thereby diluting the benefit of the structural correction’s diagonally aligned gradients for patches.

In this case, the effective mixing appears as  $\mathbf{M}_{pk} = \tilde{x}_{ke} \tilde{x}_{pe} + 1_{kp}$ , which could be counteracted using a pseudo-root-inverse of the patchwise Gram-like divergence on the forward pass; however this is computationally prohibitive and disrupts the spatialised nature of convolution. This intertwines patches non-locally, directly violating the foundational inductive-bias considerations that motivate convolution. It also breaks the translational<sup>7</sup> equivariance by introducing inter-patch mixings; although contrary to common belief this is less troublesome since edge-effects break it anyway. Nevertheless, locality of convolution would not hold. Hence, the network may be sensitive to patchwise mixing, and overall, this is conceptually unappealing. Incidentally, the often successful BatchNorm respects locality, as does the element-wise form of activation functions typically used in convolution — perhaps suggestive of BatchNorm’s empirical success in convolution.

Overall, both the prior straightforward structural corrections for batched-affine can be applied individually to patches, but their use is unsupported due to approximation breakdown due to the strong nonlinear computations interconnecting patches downstream. Similarly, full corrections are unfavourable because they undermine the inductive biases of convolution. Therefore, despite remedies for the ideal-effective misalignment theoretically existing and directly comparable to batched-affine corrections, they may be troublesome due to pathological interactions arising downstream.

Nevertheless, one can still implement PatchNorm as shown in *Figs. 8 and 9*. These are insightful examples, as despite PatchNorm being structurally identical to the batched-affine case, the implicit assumptions fundamentally differ, and subsequent outcomes are markedly different.

Overall, these results may be surprising, since superficially PatchNorm is identical to the affine divergence correction, which was previously shown to work well but did not outperform other normalisers in convolutional testing. This directly indicates the breakdown of the single-sample-like approximation, more appropriately the single-patch approximation for convolution, which held over prior batched affine experiments. Hence, such a result is conceptually significant. This suggests that these interactions cannot be neglected in approximation, a suggestion directly supported by the empirical results. As discussed, this is likely due to either non-linear mixing of patches, repeated numerical values in the unfolding, or differences in backpropagated gradients from activation to activation arising from repeated unfolding values. The explanation may be one of or a combination of these factors, as these are how convolution differs from the batched-affine success. Whether this interpatch dependency also explains why convolution *typically* empirically favours BatchNorm over other normalisers, and why this differs from affine networks, may be explored in this multi-patch ideal-effective consideration, as BatchNorm may offer a better mitigation here perhaps due to  $\text{Var} \|\tilde{x}\|^2$  damping.

From *Fig. 8* and *9*’s foundation, empirically validating the breakdown of the patch-interdependence assumption, one could explore other modes for ideal-effective alignment in representation updates for convolution. This may yield alternative, perhaps empirically more successful, normalisers using this approach. Additionally, such an effort would provide an independent route to verifying or falsifying this ideal-effective update principle for the success of normalisation. Nor should this suggest a problem with the ideal-effective misalignment theory at this stage, since PatchNorm does not adequately resolve it due to the breakdown of such assumptions. However, overall, it appears that generalising the ideal-effective misalignment theory to convolution may require substantial further, nuanced considerations to construct functions that produce approximations that better respect the construction of convolutional layers, and this is encouraged for future work.

<sup>7</sup>Really more like a special subset of permutations with respect to neurons *not* data. As ‘translation’ in this sense is more like a reindexing as opposed to translating the activation value  $\tilde{a}' = \tilde{a} - \tilde{t}$ .

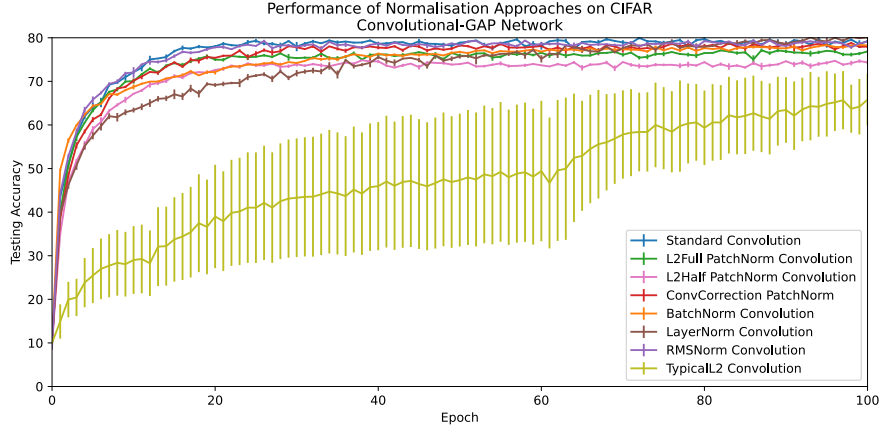


Figure 8: Shows the testing accuracy of a convolutional network, using a global average pool layer, trained for 100 epochs on CIFAR-10. Shown is the mean and standard error on accuracy for various normalisers across 5 repeats. In this plot, one can observe that LayerNorm, no Normalisation, and RMSNorm perform comparably and are the best among the comparisons. Followed, with a minimal margin, by affine-like PatchNorm and BatchNorm. After these, the  $L_2$ -PatchNorms with  $\eta$  and  $\eta/2$  perform next best, with typical (Layer-wise)  $L_2$ -norm performing more poorly. This indicates that, despite being arithmetically identical to the affine structural solutions, PatchNorm’s performance is not superior to that of other normalisers — being comparable to BatchNorm in these tests. However, all of these are parameterless formulations for ablation testing, which may account for non-standard results.

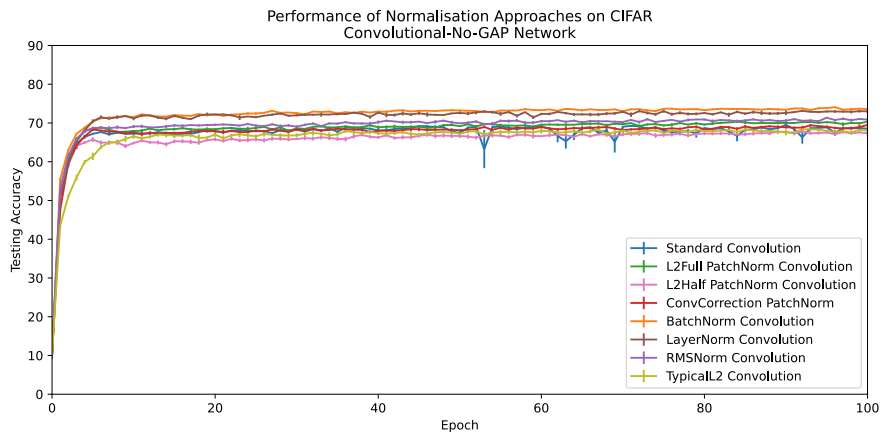


Figure 9: Shows the testing accuracy of a convolutional network, without using a global average pool layer, but instead gradually spatially reducing the activations into channels. This network is trained identically to that in Fig. 8, differing only in its architecture. This plot also shows the mean and standard error across. In this plot, one can observe that BatchNorm then LayerNorm outperform other normalisers with a large margin. This is followed by RMSNorm,  $L_2$ -PatchNorm- $\eta$ , then the affine-like-PatchNorm (red), then no normalisation, followed by  $L_2$ -PatchNorm- $\eta/2$  and  $L_2$ -LayerNorm. The difference between the two  $L_2$ -PatchNorms suggests that this test is sensitive to the learning rate, and this should be optimised for better performance. All of these results are also parameterless formulations for ablation testing, which may account for non-standard results.

Secondly, this may not be a fundamental weakness of the novel functional form of PatchNorm, which may be improved with additional parameters, such as those used in traditional normalisers. The two approaches to PatchNorm may continue to have specific use cases where they are beneficial, and a general investigation of the functional form, e.g., Patchwise normalisation, is strongly encouraged as an alternative to explore compared to existing forms.

In conclusion, despite the convolution case being structurally identical to the batched-affine case, the interpretation is significantly different due to the presence of a single sample and downstream patchwise nonlinear interdependencies, which undermine the structural solutions previously found successful in analogous batched-affine tests. This is borne out in the experiments, where structural corrections do not outperform alternative normalisers and are instead comparable or worse, depending on the normaliser. This reinforces the point that patches are not independent samples, in which samples contribute linearly and independently to the final loss; inter-patch considerations are highly non-linear and cannot be neglected without global consequences for performance. This motivates a future search for convolutional structural corrections that more accurately account for the ideal-effective misalignment to assess the validity of this mechanism.

### B.3 Residual Divergence

Residual models directly complicate the approximation assumptions asserted throughout this work. The purpose of this work was to explore whether simple corrections that reduced the affine divergence could improve performance, which, in turn, naturally yielded normalisation-like maps that offered insight into their success.

This hinged on single-layer assumptions to offer computationally straightforward and reasonably unburdensome operations that mitigate the divergence in single layers. Residual networks do not uphold this single-layer picture of interactions; they directly transmit gradients between layers using an identity map, in combination with whatever other operation is present. This directly breaks down the simple single-layer approximation being proposed and significantly complicates the divergence, which itself is strongly dependent on the function that the residual skip bypasses (often nonlinear). Consequently, pursuing residual ideal-effective divergences and structural corrections may be an interesting direction for future work, but it remains out of scope for the current approach.

### B.4 Attention Divergence

Taking the correlation step of attention to be the expression in *Eqn. 49*, with  $\mathbf{X} \in \mathbb{R}^{t \times d}$  being the stacked token vectors,  $\mathbf{W}^{(Q)} \in \mathbb{R}^{n \times d}$  and  $\mathbf{W}^{(K)} \in \mathbb{R}^{n \times d}$  being the query and key matrices, with  $\mathbf{Y} \in \mathbb{R}^{t \times t}$  respectively. Downstream activation functions, ‘values’ term and multiple heads are suppressed for notational simplicity but trivially extendable from the equations below.

$$Y_{ts} = W_{ip}^{(K)} W_{iq}^{(Q)} X_{tq} X_{sp} \quad (49)$$

From these the respective gradients can be computed with  $\frac{\partial \mathcal{L}}{\partial \mathbf{Y}} \equiv \mathbf{g}$ .

$$\frac{\partial \mathcal{L}}{\partial W_{nm}^{(Q)}} = g_{ts} W_{np}^{(K)} X_{tm} X_{sp} \quad (50)$$

$$\frac{\partial \mathcal{L}}{\partial W_{nm}^{(K)}} = g_{ts} W_{nq}^{(Q)} X_{tq} X_{sm} \quad (51)$$

$$\frac{\partial \mathcal{L}}{\partial X_{nm}} = g_{ns} W_{ip}^{(K)} W_{im}^{(Q)} X_{sp} + g_{tn} W_{im}^{(K)} W_{iq}^{(Q)} X_{tq} \quad (52)$$

(53)

Now we can substitute these as a gradient descent update step to determine the effective update on  $\mathbf{X}$ .

$$Y'_{ts} = \left( W_{ip}^{(K)} - \eta g_{de} W_{if}^{(Q)} X_{df} X_{ep} \right) \left( W_{iq}^{(Q)} - \eta g_{ab} W_{ic}^{(K)} X_{aq} X_{bc} \right) X_{tq} X_{sp} \quad (54)$$

Expanding and simplifying yields, and using  $W_{nm}^{(Q2)} = W_{in}^{(Q)} W_{im}^{(Q)}$  and  $W_{nm}^{(K2)} = W_{in}^{(K)} W_{im}^{(K)}$  and  $X_{nm}^{(g2)} = g_{ab} X_{an} X_{bm}$ , yields *Eqn. 55*, the ‘attention divergence’.

$$Y'_{ts} = Y_{ts} - \eta \left( W_{qf}^{(Q2)} X_{fp}^{(g2)} + W_{pc}^{(K2)} X_{cq}^{(g2)} \right) X_{tq} X_{sp} + \eta^2 \left( W_{ic}^{(K)} W_{if}^{(Q)} X_{fp}^{(g2)} X_{qc}^{(g2)} \right) X_{tq} X_{sp} \quad (55)$$

We can compute the solution, which must be normalisation-like due to the lack of bias, given by *Eqn. 56*. However, this can be applied, vector-wise,  $s_i$  or  $s_p = s_q$ , token-wise,  $s_t = s_s$  or globally,  $s$ . Proceeding globally with scalar  $s$ .

$$Y_{ts} = \frac{W_{ip}^{(K)} W_{iq}^{(Q)} X_{tq} X_{sp}}{s} \quad (56)$$

Recomputing gradients yields:

$$\frac{\partial \mathcal{L}}{\partial W_{nm}^{(Q)}} = \frac{g_{ts} W_{np}^{(K)} X_{tm} X_{sp}}{s} \quad (57)$$

$$\frac{\partial \mathcal{L}}{\partial W_{nm}^{(K)}} = \frac{g_{ts} W_{nq}^{(Q)} X_{tq} X_{sm}}{s} \quad (58)$$

$$\frac{\partial \mathcal{L}}{\partial X_{nm}} = \frac{g_{ns} W_{ip}^{(K)} W_{im}^{(Q)} X_{sp} + g_{tn} W_{im}^{(K)} W_{iq}^{(Q)} X_{tq}}{s} \quad (59)$$

(60)

Then substituting yields *Eqn. 61*

$$Y'_{ts} = Y_{ts} - \eta \left( \frac{W_{qf}^{(Q2)} X_{fp}^{(g2)} + W_{pc}^{(K2)} X_{cq}^{(g2)}}{s^2} \right) X_{tq} X_{sp} + \eta^2 \left( \frac{W_{ic}^{(K)} W_{if}^{(Q)} X_{fp}^{(g2)} X_{qc}^{(g2)}}{s^3} \right) X_{tq} X_{sp} \quad (61)$$

Then one can attempt a solution for  $s$  under various assumptions. In this approach, it will be assumed that  $\eta^2 \rightarrow 0$  and using the ideal gradient of  $g_{ts}$ .

$$g_{ts} = -g_{kl} \frac{W_{qa}^{(Q2)} X_{tp} X_{sq} + W_{pa}^{(K2)} X_{tq} X_{sp}}{s^2} X_{ka} X_{lq} \quad (62)$$

$$\delta_{kt} \delta_{ls} = -\frac{1}{s^2} \underbrace{\left( W_{qa}^{(Q2)} X_{tp} X_{sq} + W_{pa}^{(K2)} X_{tq} X_{sp} \right)}_{g_{kts}^*} X_{ka} X_{lq} \quad (63)$$

This correction, even with the stated assumptions, appears highly non-trivial and perhaps intractable in general, even before considering the subsequent values step and multiple stacked heads. Therefore, this generalisation will not be pursued at the current time for attention mechanisms.

Whether this partially explains the absence of normalisation in attention layers is an interesting speculation. In such cases, standard normalisation would not reduce the attention divergence as it does for affine maps; consequently, any empirical advantage may be absent. Perhaps this has implicitly suppressed the use of normalisation here, although the conceptual undesirability of normalisation here and its interactions with softmax may be additional significant reasons for its absence. Future work could elucidate this by examining whether approximate corrections to the divergence are possible or whether typical normalisers help mitigate this, yielding improved performance.